JANUARY 2018

M.Sc. in Civil Engineering

KOCHAR DARA MOHAMMED

UNIVERSITY OF GAZİANTEP

GRADUATE SCHOOL OF

NATURAL & APPLIED SCIENCES

INVESTIGATION OF EFFECT OF INTERMEDIATE SILL ON LOCAL SCOURING AT THE END OF STILLING BASIN

M. SC. THESIS

IN

CIVIL ENGINEERING

BY

KOCHAR DARA MOHAMMED

JANUARY 2018

Investigation of Effect of Intermediate Sill on Local Scouring at the End of Stilling Basin

M.Sc. Thesis

in

Civil Engineering

University of Gaziantep

Supervisor

Prof. Dr. Mustafa GÜNAL

by

Kochar Dara MOHAMMED

January 2018

REPUBLIC OF TURKEY
UNIVERSITY OF GAZİANTEP
GRADUATE SCHOOL OF NATURAL & APPLIED SCIENCES
CIVIL ENGINEERING DEPARTMENT

Name of the thesis: Investigation of Effect of Intermediate Sill on Local Scouring at the End of Stilling Basin

Name of the student: Kochar Dara MOHAMMED

Exam date: 04/01/2018

Approval of the graduate school of natural and applied science.

Prof. Dr. Ahmet Necmeddin YAZICI
Director

I certify that this thesis satisfies all the requirements as a thesis for the degree of Master of Science.

Prof. Dr. Abdulkadir ÇEVİK
Head of Department

This is to certify that we have read this thesis and that in our consensus opinion it is fully adequate, in scope and quality, as a thesis for the degree of Master of Science.

Prof. Dr. Mustafa GÜNAL
Supervisor

Examining Committee Members:	Signature
Prof. Dr. Mehmet KARPUZCU	....
Prof. Dr. Mustafa GÜNAL	....
Prof. Dr. Aytaç GÜVEN	....

I hereby declare that all information in this document has obtained and presented in accordance with academic rules and ethical conduct. I also declare that, as required by these rules and conduct, I have fully cited and referenced all materials and results that are not original to this work.

Kochar Dara MOHAMMED

ABSTRACT

INVESTIGATION OF EFFECT OF INTERMEDIATE SILL ON LOCAL SCOURING AT THE END OF STILLING BASIN

MOHAMMED, Kochar Dara
M.Sc. in Civil Engineering
Supervisor: Prof. Dr. Mustafa GÜNAL
January 2018
62 pages

In this study, a three-dimensional numerical model of sediment was simulated based on previous experimental work. The simulation was performed by using Flow-3D software the Renormalized Group (RNG) k-ε turbulence model was chosen in the numerical modeling. The scour process was calculated at the end of the USBR type VI stilling basin with impact wall, end sill and intermediate sill. To investigate the effect of intermediate sill geometry on the local scour depth, four different intermediate sill geometry were used and maximum scour depth for each model was simulated at the end of stilling basin to select the best type of intermediate sill that reduces the scouring to a minimum value. To assess the precision of the CFD program the numerical results will be compared with experimental. After the simulation, the results showed that the numerical results close to the experimental, but only had the high difference in model-5. Results showed that intermediate sill has a great effect on the scour depth at the end of the stilling basin, it has a clear difference between the results of scour depth for stilling basin with and without intermediate sill and their effects depend on it is geometry, the results showed that the minimum scour depth occurred in the square intermediate sill.

Key words: Local scour, Flow-3D, Intermediate sill, Stilling basin

ÖZET

ENERJI KIRICI HAVUZLARDA BLOK ETKISININ OLUŞAN YEREL OYULMA ÜZERINDEKI ETKISININ ARAŞTIRILMASI

MOHAMMED, Kochar Dara
Yüksek Lisans Tezi, İnşaat Mühendisliği Bölümü
Danışman: Prof. Dr. Mustafa GÜNAL
Ocak 2018
62 sayfa

Bu çalışmada, önceki deneysel çalışmaya dayanılarak üç boyutlu sayısal bir malzeme taşınım modellemesi yapılmıştır. Modelleme, Flow-3D yazılımı kullanılarak gerçekleştirilmiştir. Renormalize Grup (RNG) k-ε türbülans modeli sayısal modellemede seçildi. Yerel oyulma, USBR tip VI enerji kırıcı havuzun sonunda darbe tutucu duvar, son eşik ve ara eşik kullanılarak modelleme yapıldı. Orta eşik geometrisinin yerel oyulma derinliği üzerindeki etkisini araştırmak için, dört farklı ara geçiş geometrisi kullanıldı ve her model için maksimum oyulma derinliği, enerji kırıcı havuzun sonunda, oyulma işlemini en aza indirgeyen ara eşiğin en iyi tipini seçmek üzere modelleme yapıldı. Minimum değer. CFD programının hassasiyetini değerlendirmek için sayısal sonuçlar deneysel sonuçlar ile karşılaştırıldı. Modellemeden elde edilen sonuçlar, sayısal sonuçların deneysel olana yakın olduğunu, ancak sadece Model 5'de yüksek fark olduğunu gösterdi. Sonuçlar, orta eşiğin, enerji kırıcı havuzun sonundaki oyulma derinliği üzerinde büyük bir etkiye sahip olduğunu, ara eşiğin bulunduğu ve bulunmadığı enerji kırıcı havuzun sonunda oluşan oyulma derinliğinin sonuçları arasında net bir fark olduğunu ve etkilerinin geometriye bağlı olduğunu, minimum oyulma derinliğinin kare şeklindeki orta eşiğin oluşturduğunu gösterdi.

Anahtar Kelimeler: Yerel oyulma, Flow-3D, Ara eşik, Enerji kırıcı havuz.

To

My parents

ACKNOWLEDGEMENT

I would like to express my special appreciation and thanks to my supervisor Prof. Dr. Mustafa GÜNAL, for all his help, patience, valuable advice, always providing and guiding me in the right direction. I'm very grateful and proud to work under her academic guidance.

Special thanks to my family. Words cannot express how grateful I am to my father spirit that his words lead me to get certificates and my mother for all of the sacrifices that have made on my behalf. Also to all my sisters and brothers, for their strong encouragement during the years of my study.

TABLE OF CONTENTS

Page

LIST OF TABLES

Page

LIST OF FIGURES

Page

LIST OF SYMBOLS/ABBREVIATIONS

SB	Stilling Basin
USBR	United States Bureau of Reclamation
CFD	Computational fluid dynamics
ICOLD	International Commission on Large Dams
RNG k-ε	Renormalized group k-ε
u_i'	fluctuation of fluid velocity in i direction
u$_i$	fluid velocity component in i direction
$\overline{u_i'u_j'}$	Reynolds stress tensor
P	Pressure
ρ	Fluid density
v_t	Turbulence viscosity,
S_{ij}	Mean strain rate tensor
v	Fluid kinetic viscosity
k	Turbulent kinetic energy
δ_{ij}	Kronecker delta
ε_T	Rate of turbulent energy dissipation
ε	Dissipation of turbulent kinetic energy
μ_t	Turbulent eddy viscosity

τ_{ij}	Reynolds stress
VOF	Volume of fluid
FAVOR	Fractional Area / Volume Obstacle Representation
VF	Volume fraction
AF	Area fraction
R_{DIF}	Turbulent diffusion
R_{SOR}	Mass source
A_y	Area fractions for flow in the y direction
A_z	Area fractions for flow in the z direction
stl	stereolithographic

CHAPTER 1

INTRODUCTION

1.1 General

Open channel flow with erodible bed generally includes the transport of sediment particles (Raudkivi, 1967). Scour can occur in a result of a flow change in the flow path or due to an artificial activity such as the construction of water control structure within the flow path or dig up of substances from the bed. This mechanism has the potential threat to the integrity of the hydraulic structure and eventually may be cause for the failure of the structures when the foundation is undermined. The natural occurrence due to the flow of water over an erodible is called scour (Breusers et. al.,1977).

The erosion of sediment which takes place near the water control structure, exposing the foundation of the structure and then it may be damaged Barlock (2013). Flow intensity and many properties of the sediment particle are effected on erosion rate such as density, gradation and size. The first equation of sediment transport was developed by Gilbert (1914) then many equations have been proposed for multi or single grain sized sediment in steady uniform open channel flow.

Some of these equations refer to the total sediment load, which bed load and suspended load are not distinguished or are only for suspended load or bed load, the total load equations are most commonly used by engineers Acharya (2011).

Commercial Computational Fluid Dynamic (CFD) code provides a reasonable way to predict scour phenomena, however, most programs do not accommodate scour models in hydraulic systems due to the difficulty of the scouring process. Flow-3D proposed by (Flow Science Inc.) has excellent ability to solve scour problems, however, the sediment transport model is based on empirical formulas which increases the computation time and makes it impossible to complete several simulations within a reasonable time.

At the end of the water control structures like pipe outlets, spillways, sluice gates, and culvert due to the excess kinetic energy of flowing water Stilling Basin (SB) is used to dissipate this energy in order to protect the structure as shown in Figure 1.1. The main purpose in the use of the SB is to decrease a scour depth and localize it in a location that can be controlled or minimizing the scour hazards on the stability of the structure, eliminate of the scour is almost impossible especially uneconomic. The development and depth of the local scour be influenced by parameters such as hydraulic structure, geological and basin geometry (Annandale, 1995).

Different types of appurtenances are used, for any SB type appurtenances have an important role in reducing the energy of moving water. SB for a pipe outlet uses appurtenances such as end sill, splitter block, intermediate sill and impact wall.

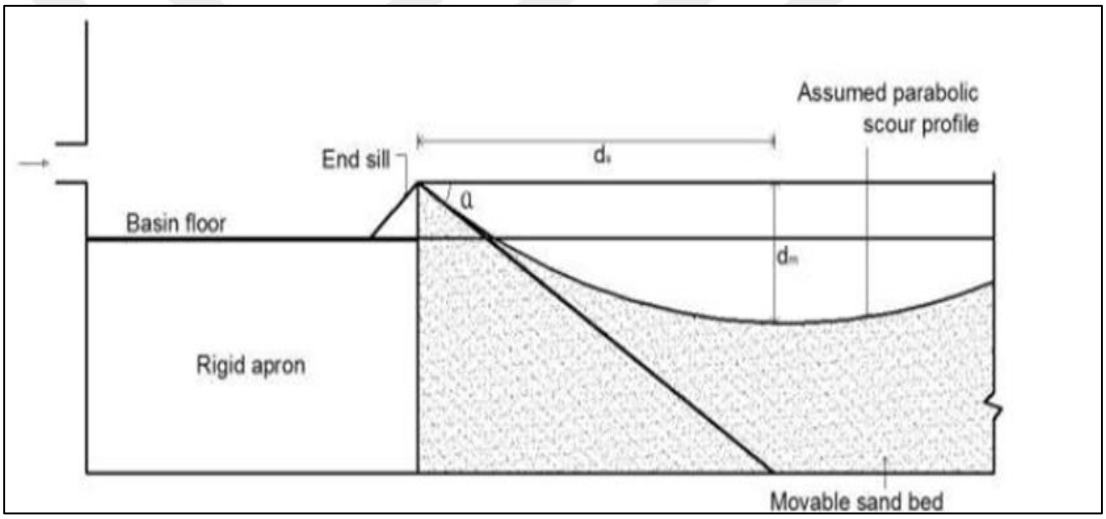

Figure 1.1 Assumed scour pattern (Tiwari,2013)

The sill serves to reduce the length of the hydraulic jump and minimize the scour, scour characteristics is affected by sill geometry, position and the flow regime. Negm (2004) performed a laboratory investigation to observe the effect of sill arrangements on the appearances of scour downstream of the basin was determined that the scour depth at the of the SB is greatly affected by using the sill inside the basin.

Saleh et. al. (2004) performed a laboratory investigation on the effect of asymmetrical side sill from both single and double side sills to minimize the depth of the scouring downstream of the suddenly expanding SB. Five different positions of asymmetrical side sill were tested the maximum scour depth is significantly reduced by single and double-sided sills.

The statistical researchers in the last decades had presented that the most extensive cause of failure in bridges is the erosion of materials above their foundations. In 1973 Federal Highway Administration of USA investigated 383 bridge failures, which were resulted from great damaging floods (Federal Highway Administration, 2001).

In Turkey during the last decades, some floods occurred which caused the failure of these bridges: Trabzon (1990), Malatya (1991), Bartın (1998), Hatay (2001), and Mersin (2001) (Yanmaz, 2002) because of removing of bed materials around bridge foundations.

1.2 Scour

Scour is the process of erosion of particles from the channel bed and bank caused by water flow (Ebrahim and Heydarnejad, 2014). Scour can cause serious engineering and environmental problems, the most common causes of bridge failure during floods are the erosion of particles on the foundation Xie (2011).

For estimating scour has numerous equations based on laboratory experiments with limit validation from field investigation, whereas uncertainty in predicting scour still remains, the proposed equations is currently considered to be the best existing method for determining the depth of scouring (Bridge Scour Manual, 2013).

Scour process possibly will gradually damage the bed protection downstream of the structures (M. A. Khalifa and Kh. A. Zahra, 2014). Since bed protection also fails over time, we need to find the best solution that is economical and durable to extend the service life of the engineering infrastructure.

1.3 Types of Scour

Scour is classified into two main types:

a) General scour

b) Localized scour, as illustrated in Figure 1.2.

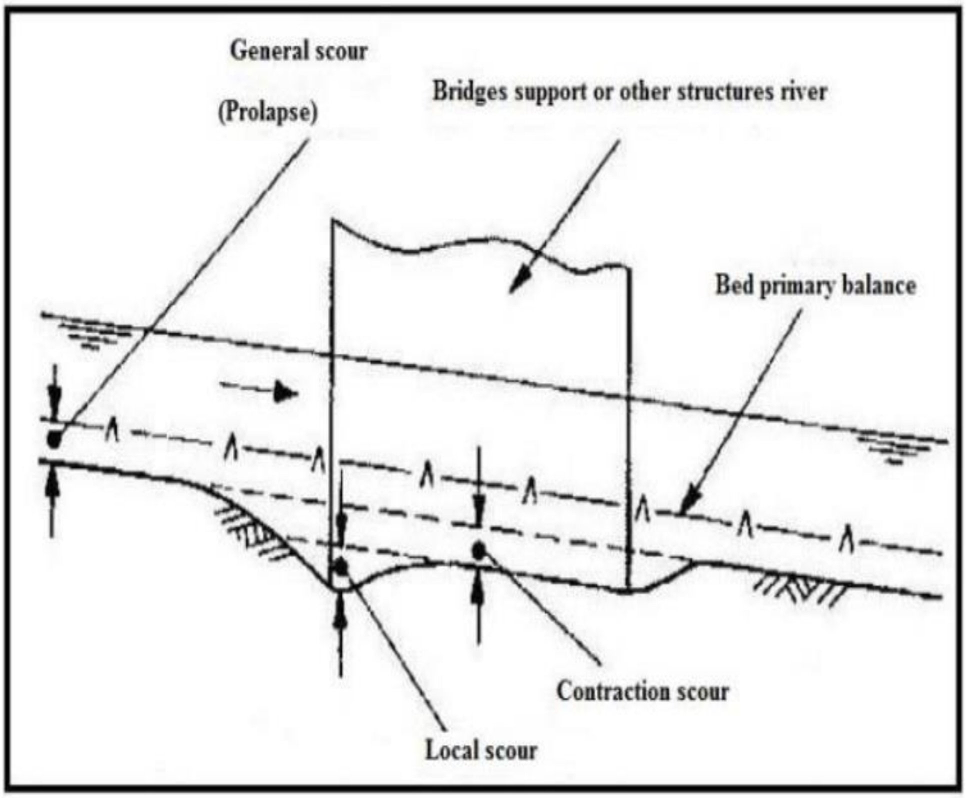

Figure 1.2 Types of scour

1.3.1 General scour

This type of scour includes the erosion of the materials from bed and banks through all or most of the width of a channel. General scour can be due to natural or artificial causes and requires both geomorphologic and sediment analysis Kayaturk (2005).

1.3.2 Localized scour

Localized scour is further divided into contraction and local scour:

1.3.2.1 Contraction scour

This type of scour takes place when a flow path in the channel is reduced by natural or artificial causes. With a decrease in the cross sectional area, as a result an increase in average velocity and shear stress occurs, this may cause the erosion of more sediment material and thus a total lowering of the bed elevation happened in the contracted area this type of scour is known as contraction scour Johnson (2005).

1.3.2.2 Local scour

Local scour is regarded as lowering of the bed close to the structure due to the local acceleration of near bed velocity and associated turbulence (vortices), which increases the local transport rate. Excessive scouring near to the structure may eventually lead to the damaging of the structure (Leo C. van Rijn, 2013)

1.4 Research Purpose

The aim of this study is to simulate a numerical model based on the experimental study by Tiwari et al. (2014). To observe the effect of the intermediate sill on local scouring at the end of SB, and determining the best geometry of intermediate sill that reduces scouring to the minimum value, the simulation is performed by using Flow-3D software, then comparing the results with experimental studies to assess the precision of Flow-3D software in simulating scouring model.

1.5 Layout of the Thesis

The research consists of five chapters. A brief review of each chapter is explained as follows:

Chapter 1 Introduction:

Present a simple history of common scouring phenomena and further clarify research purpose and layout of the research.

Chapter 2 Literature Review:

In this chapter, we will discuss the initiatives that deal with sediment scouring at the end of hydraulic structures, empirical equations in the numerical model, numerical methods, a previous study of both physical and numerical methods about scouring.

Chapter 3 Case-Study:

The experimental and numerical modeling will be explained in this chapter, sediment transport modeling in Flow-3D, and set up numerical modeling.

Chapter 4 Results and Discussion:

In this chapter, will be showing the numerical results and compares with physical results to access the reliability of Flow-3D program for simulating the scour model also the best geometry of intermediate sill that reduces the scour to minimum value will be selected then the effect of flow depth, Froude number, vorticity and velocity on scouring will be discussing.

Chapter 5 Conclusions:

This section briefly introduces the most important conclusions of both numerical and experimental studies, showing the similarity of both studies, the effect of sill in reducing scouring and gives information about the best geometry of intermediate sill.

CHAPTER 2

LITERATURE REVIEW

2.1 General

Erosion and sedimentation is the motion process of solid particles during geological time. It is form the present landscape, morphology and can cause severe engineering and environmental problems. For example, erosion can cause on site damage to the agricultural land, reduce the productivity of fertile soils and cause local scour problems along with serious sedimentation downstream of the hydraulic structure. Due to advances in computer processing capacity, research to deal with scouring problems which used numerical techniques had increased recently. Numerical investigations have been applied extensively to describe the nature of the flow field and the local scouring. The researchers simulated an erodible bed to model the sediment transportation. In this study commercially available CFD program FlOW-3D software has been used to solve flow field and scour problem.

The computational sediment transport models comprise the numerical resolution of a chain of governing differential equations such as energy coupled with the interaction of sediment particles, fluid in the computational domain, continuity equation and momentum equation

2.2 What is Stilling Basin

Stilling basin is located at the end of water control structures such as dam spillway, culvert outlet, pipe outlet and sluice gate. In such cases, it is used to dissipate the excess energy of water that falls from the upper portion of the structure to lower portion.

SB is used chiefly to protect the water control structure from any expected failure because of the erosive force of the high velocity jet, many types of SB were discussed in the literature, United States Bureau of Reclamation (USBR) stilling basin is one of these basin types. Dissipation of energy is necessary to keep the structure safety because the excess energy will cause extra scouring at the end of hydraulic structure, then undermine the foundation of the structure and may cause to damage of it eventually, to protect against this problem a reasonable way is the use of concrete paved SB, there are many basin types that are used to dissipate energy Plaza et. al. (2014).

A suitable energy dissipater must be able to dissipate the high energy of flowing water in a way that protects the structure and channel from damaging Wei (1999). In previous researchers conducted numerous experimental, field and numerical investigation to obtain a suitable energy dissipator and their publications still used and widely referenced (United State Bureau of Reclamation (USBR), 1987; International Commission on Large Dams (ICOLD), 1987) and Hendreson, 1966). There are two main types of energy dissipator: hydraulic jump type dissipator an impact type dissipator:

2.2.1 Hydraulic jump stilling basin

In this type of energy dissipator excess energy dissipate through the formation of highly turbulent rollers within the jump, the hydraulic jump basin is usually used for energy dissipation in the downstream side of water control structure and prevents scouring Mays (1999). The hydraulic jump SB type dissipates about 10 to 85 percent energy, which considered on the velocity and depth of the arriving water and available tail water depth (Tiwari et al. 2010).

A jump in water pressure is a natural phenomenon that occurs from the transition of a supercritical flow to a subcritical flow. This is a sudden change in the state of the flow, is achieved by turbulence and energy loss which makes, the hydraulic jump an efficient way of dissipating energy.

Hydraulic jump SB effectively dissipates energy, but it required a large length if there is for basin without an obstruction as shown in Figure 2.1. From an economic point of view, it is necessary to restrict the entire jump by a various specific structure as end sill, baffle blocks, and chute blocks. To increase turbulence and stabilization of the jump these appurtenances are added thereby reduce the length of the SB and providing a protection against sweep out caused by tail water depth.

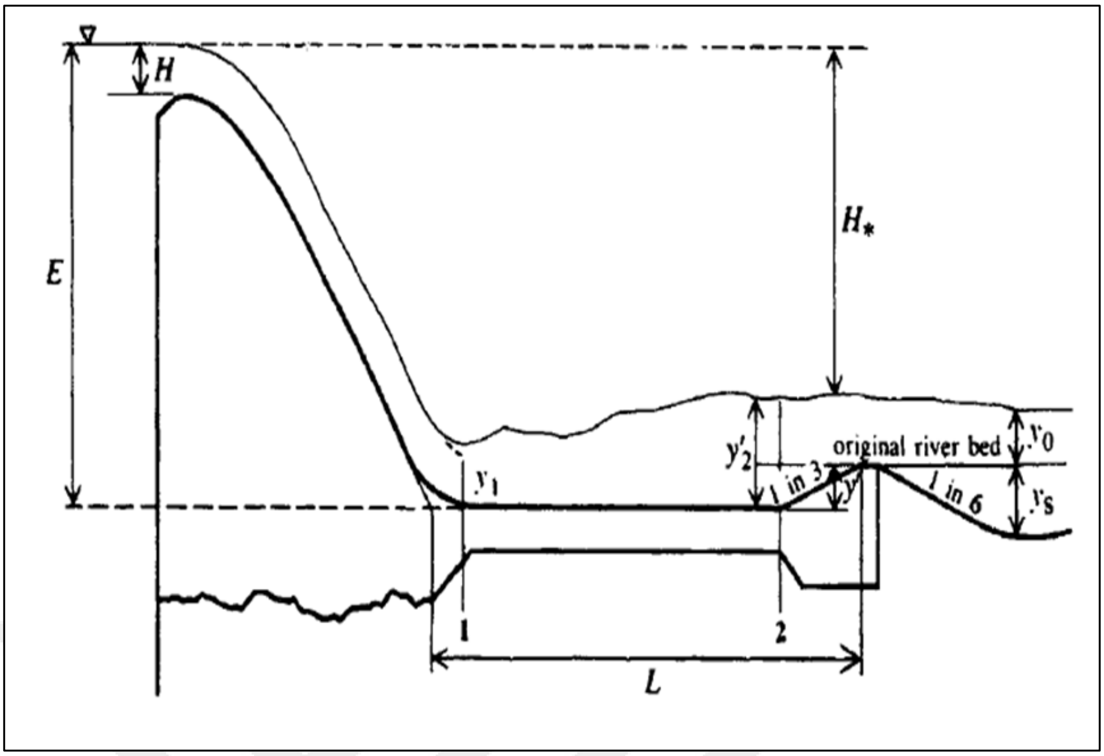

Figure 2.1 Hydraulic jump stilling basin(Novak, 2007)

2.2.2 Impact type stilling basin

The impact type SB energy dissipator direct the water into an obstacle that divides the water in all directions and creates high levels of turbulence by this way dissipates the energy of water this structure is called impact wall as in Figure 2.2. The impact-type SB include vertical drops and check drops, vertical stilling wells, baffled aprons and baffled outlets. Commonly, the use of an impact-type SB is more economic Mays (1999).

The impact wall blocking the free flow of water, return back the water and divide the water into all width of the basin thereby changes the downstream flow regime and dissipates energy. The shape of the basin developed from numerous experiments and resulted in a design based on a vertical hanging baffle, dissipation of energy is initiated by flow striking and deflected upstream by the impact wall which creating horizontal eddies. The most common type of impact SB is the USBR Type VI that is commonly used in highway engineering.

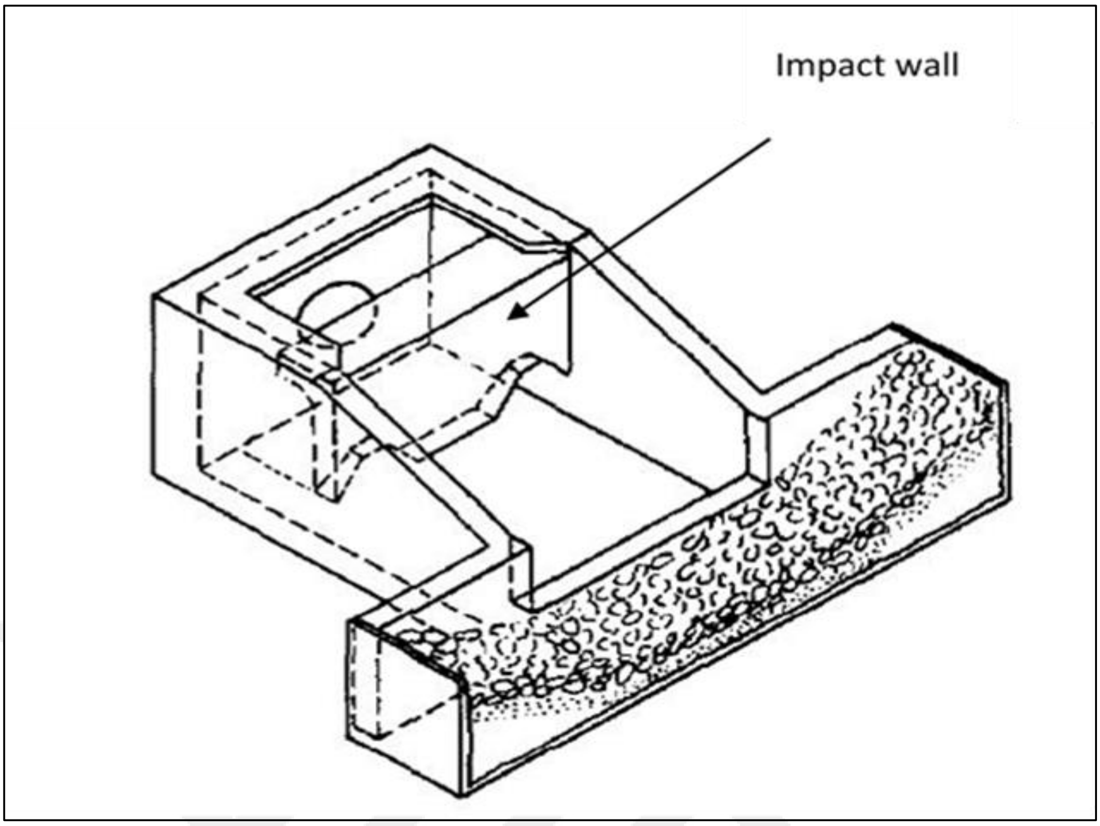

Figure 2.2 Impact type stilling basin (Peterka, 1958)

2.2.2.1 USBR type VI stilling basin

In this study USBR type SB was used, this type of basin has operational experience and is based on model studies from Reclamation (1955). It is a small structure but is more effective in dissipating energy, limited to a maximum velocity of 15 m/s and Froude numbers lower than 10 and is suitable for a discharge up to 11 m3/s. The ratio of basin width to the equivalent diameter of non circular outlet is 6.3 Olukanni et. al. (2017).

It is advanced by Bradley & Peterka (1957) energy dissipation is attained by creating a turbulence in the flowing water in the basin. The jet of water attacks against the impact wall, which distribute the flowing water over all channel width equally. Usually at the end of the USBR Type VI SB to reduce the length of the basin the end sill is located, the end sill reduces velocities in the downstream side as in Figure 2.3. Impact basin is more efficient energy dissipators than hydraulic jump basin if properly designed.

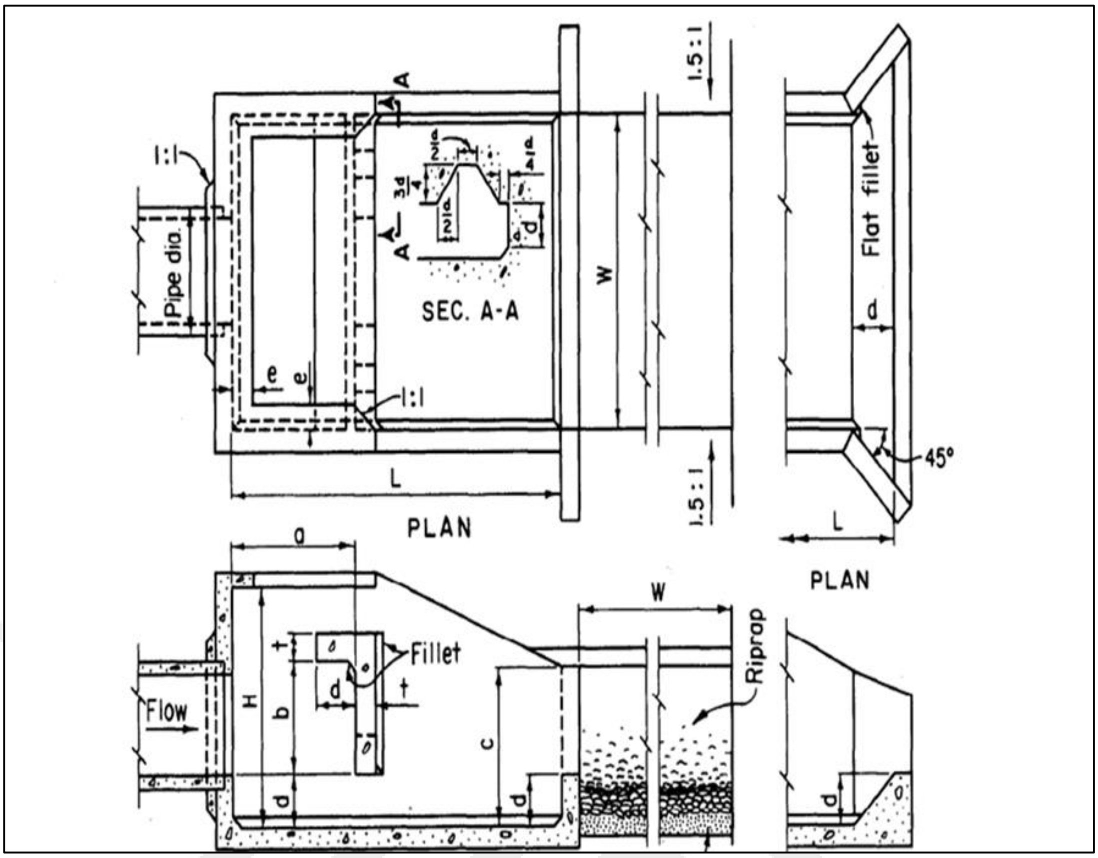

Figure 2.3 USBR type VI stilling basin (Peterka, 1958)

2.3 Studies About Stilling Basin and Sills

Sediment transportation developed over the last decades with the rapid progress of high performance computers and CFD, a calculation model of sediment transport for studying erosion in various environments such as rivers, lakes and coastal areas has become an attractive tool. The advantage of a computational model it can be more easily adopted by different physical domains of a physical model that is typically configured to represent site-specific conditions (Papanicolaou et.al, 2008).

Bharat and Tiwari (2014) studied different SB models that designed by previous researchers, they declared that appurtenances such as, intermediated sill, end sill, baffle block and impacted wall had a great effect on hydraulic energy. Mohammed et.al (2004) studied the effect of curvature and end sill angle on scour depth by using an experiment, he demonstrated that the curvature with end sill angle effects on scour depth and reduced it. From the experimental study, by changing the end sill angle from 10^o to 60^o the reduction in scour depth was obtained by 18%.

Tiwari and Arun (2014) experimentally investigated the effect of end sill on the performance of the SB in dissipating energy and reducing scouring. The research confirmed that end sill had a great effect on the performance of the SB model because it changes the flow characteristics and scour pattern of bed material was minimized.

Abdelazim et. al. (2010) studied the effect of the position of the continuous sill on velocity distribution and scour depth, the results showed that intermediate sill better than end sill in minimizing scouring.

Tiwari and Arun (2015) experimentally studied the effect of impact wall in the SB model it is concluded that the size, location and gap beneath the wall from the basin floor affect the performance of SB significantly due to changes in the flow conditions and the scour pattern downstream of the SB. It is also found that by using suitable impact wall at the appropriate location the length of the basin can be reduced to 30% as compared.

Abdelhaleem (2013) experimentally studied the effect of semicircular baffle blocks on the scouring at the weir outlet, results showed that baffle blocks had a significant influence on the scour hole, which was significantly reduced a scour.

Saleh1et.al (2003) studied a laboratory investigation on the effect of end sill in the scouring at the end of sudden expanding SB. They found that practically, the use of end sill in sudden expanding SB to reduce the scour depth is not recommended.

Tiwari1et. al. (2014) conducted a laboratory study on the effect of triangular intermediate sill height on the performance of the SB in the reducing of scouring, they found that the sill height it has a great effect on the SB performance.

de Vries (1973) studied the scouring process by using a physical and computational model to get a better understanding of the process.

2.4 Types of Scour

Erosion is one of the most potentially hazardous environmental phenomena and it has been recognized as a severe threat to the safety of the hydraulic structure. The total scour in a river channel classified into three components, such as general, local and contraction scouring (Richardson and Davies 1995).

Cheremisinoff et al. (1987) classify the total scour into two main types, general and localized scour and then subdivided these main types as shown in Figure 2.4.

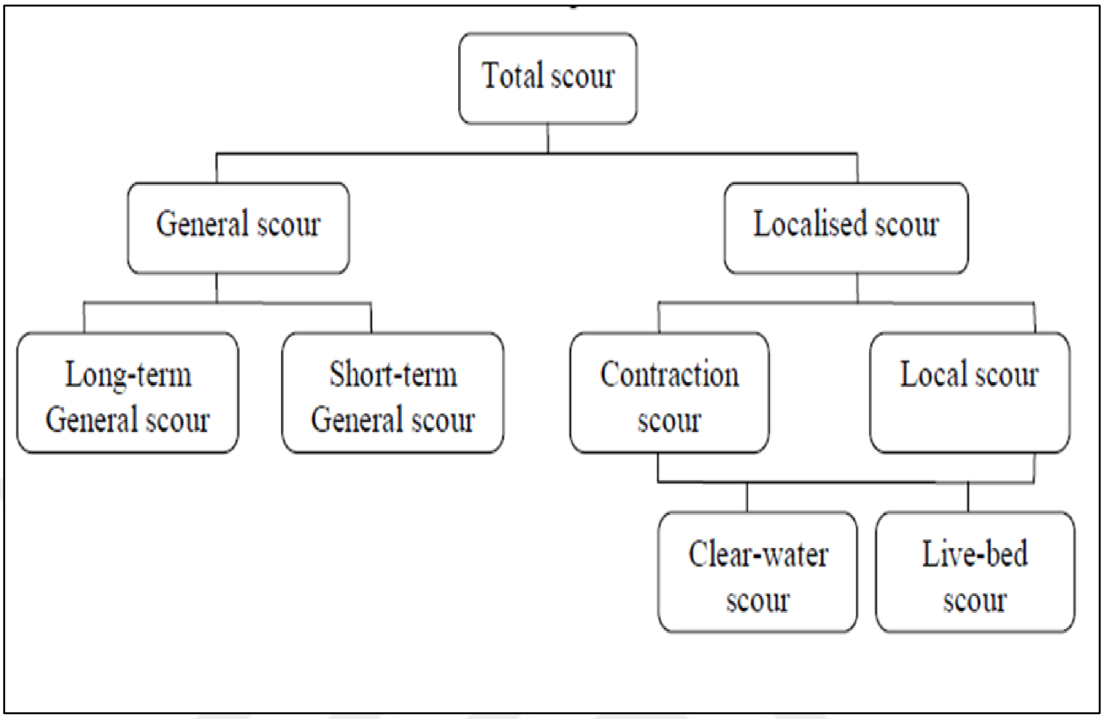

Figure 2.4 Various types of scouring modified from(Cheremisinoff et al. 1987)

2.4.1 General scour

General scouring occurs in streams and rivers because of a natural process, whether or not structures are present (Breusers & Raudkivi, 1991). The general scour function is mainly influenced by the sectional shape of the river valley. When the flow of the flood is confined, it occurs a large change in the height of the water surface and the scouring power of the flow increases (Raudkivi, 1998). General scour can be subdivided into short term and long term scour, these types of scouring can be differentiated by the temporal development of the scouring process (Cheremisinoff et al. 1987). Short term scours as a result of a single or several closely spaced floods whereas long term scour progress over a long time period, usually in the several years.

2.4.2 Localized scour

This type of scour occurred due to an obstruction in the water, and it can be subdivided into contraction scour and local scour:

2.4.2.1 Contraction scour

This type of scour occurs when the flow area is reduced due to the natural or artificial change that decreases waterway in a results an increase in velocity and bed shear stress over the contraction area is happening, therefore, the erosive forces in the contracted area increased, more bed materials are removed from the contracted region due to excessive shear stress and high velocity (Ozalp, 2013). Contraction scour subdivided into two type live bed scour and clear water according to the approaching flow.

2.4.2.2 Local scour

Local scour occurs in the river bed while there is an obstruction in the waterway that changes the state of the water flow and causes local disturbances of the flow and sediment transport field. For example, scour around (bridge) piers and abutments and scour downstream of the dam and other hydraulic structures Yildiz (2014).

Local scour happens in non-uniform flow regions, where the water is accelerated around hydraulic structure due to high velocity and bed shear stress or in regions where vortices or large eddies is occurring. Local scour is limited to a comparatively small region when comparing with the general scour, the flow field in the local scours region is disturbed and non-uniform.

The main mechanisms of local scour are:

(a) The creation of secondary flows in the form of vortices.

(b) Increased mean flow velocities and pressure gradients in the vicinity of the structure.

(c) The increased turbulence in the local flow field, two kinds of vortices may occur:
(i) Horizontal vortices at the bed and free surface due to stagnation pressure variations along the face of the structure and flow separation at the edge of the scour hole.

(ii) Wake vortices, downstream of the points of flow separation on the structure.

Shen et al. (1969) said the scouring phenomena is relatively easy to predict but is difficult to measure it mathematically.

Local scour classifies into two subdivision type, according to the type of sediment transport in the approaching channel, live bed scour and clear-water scour:

- Live bed scour: Live bed scour occurred when the approaching flow is carrying a sediment particle and transported into the scour hole. Live-bed scour usually occurs in river systems and also in recirculating flumes.
- Clearwater scour: In this type of scour, the scour hole is not refilled by the sediment particles from the approach channel while the bed particles from the scour hole are transported (Melville, 1984). In clear water scour, the equilibrium scour depth is gotten when the rate of transportation is equal to zero from the scour hole (Breusers et al. 1977). Also, clear water scour can change to live bed scour at high flows. In Figure 2.5 clear water and live bed scour are illustrated.

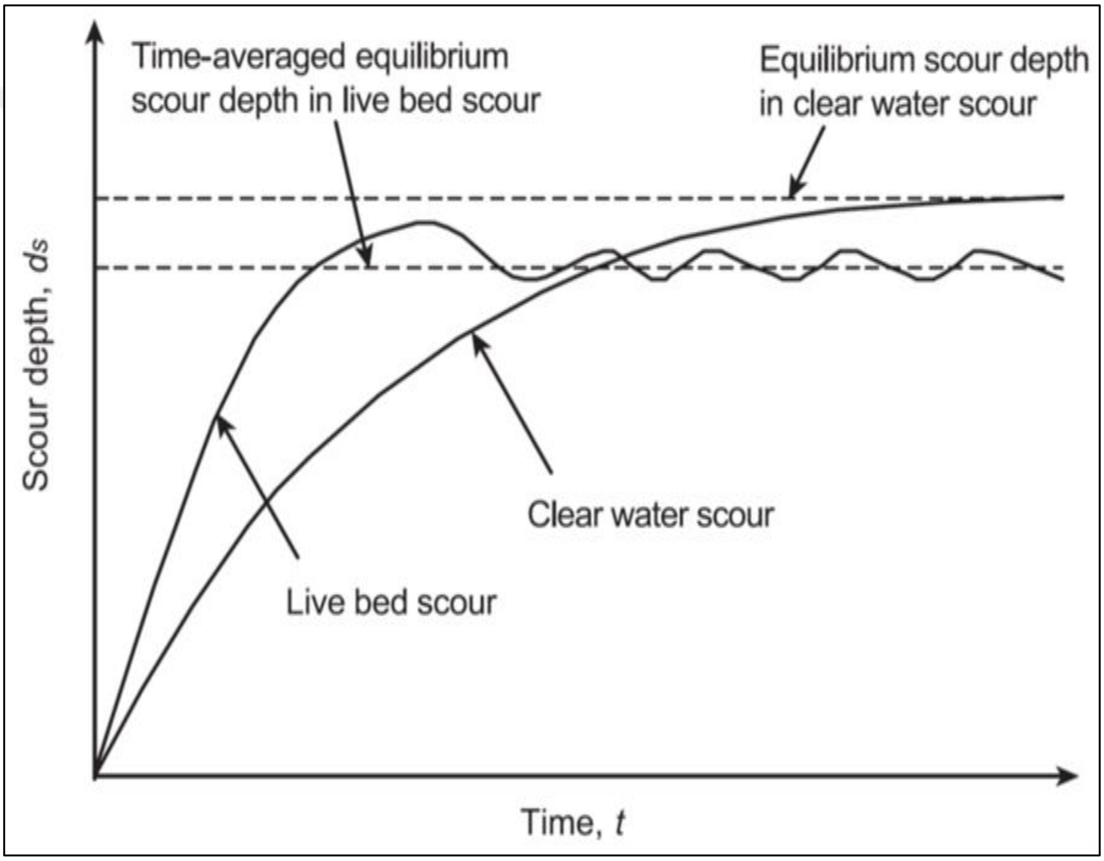

Figure 2.5 Temporal variation of the scour depth (Chabert and Engeldinger, 1956)

Hoffmans and Pilarczyk (1995) they divided the clear water scour process into four phases, initial phase, developmental phase, stabilization phase, and equilibrium phase.

- **Initial phase**

In this phase, the scour hole in the flow direction is closely uniform. This phase of the scour development can be considered as the phase that the erosion rate is most severe.

Breusers (1966) conducted an experimental investigation by using fine sediments, to observe the scouring process indicated that at the start of the scour hole formation the bed material immediately from the upstream scour slope drives into suspension.

- **Development phase**

In this phase, the scour hole developed significantly but the scour hole form it does not change. Measurements were showed that in the development phase the upstream of the scour hole gradient is in equilibrium, while the downstream part of the scour hole is still developing (Hoffmans,1990). In the recirculation zone, the suspended load near the bed is significantly reduced compared to the conditions of the initial stage. It is believed that this is mainly due to a decrease in the flow velocity near the bed in time, despite the increase in turbulent energy.

- **Stabilization phase**

In this phase, the rate of development of the scour depth decreases because of the erosion capability is very small in the bed of the scour hole when compared to the erosion capability downstream of the scour hole, the scour hole dimension more increase in the direction of the flow but a slight increase in the vertical direction. At the stabilization stage, almost an equilibrium has been achieved for the scour hole shape and a maximum depth of the scour.

- **Equilibrium phase**

This phase can be defined as a stage where the size of the scour hole no longer varies significantly as showed in Figure 2.6. Typically, at this stage of the scouring process the bed particles in the upstream scour hole gradient will only roll and slide below the salt level.

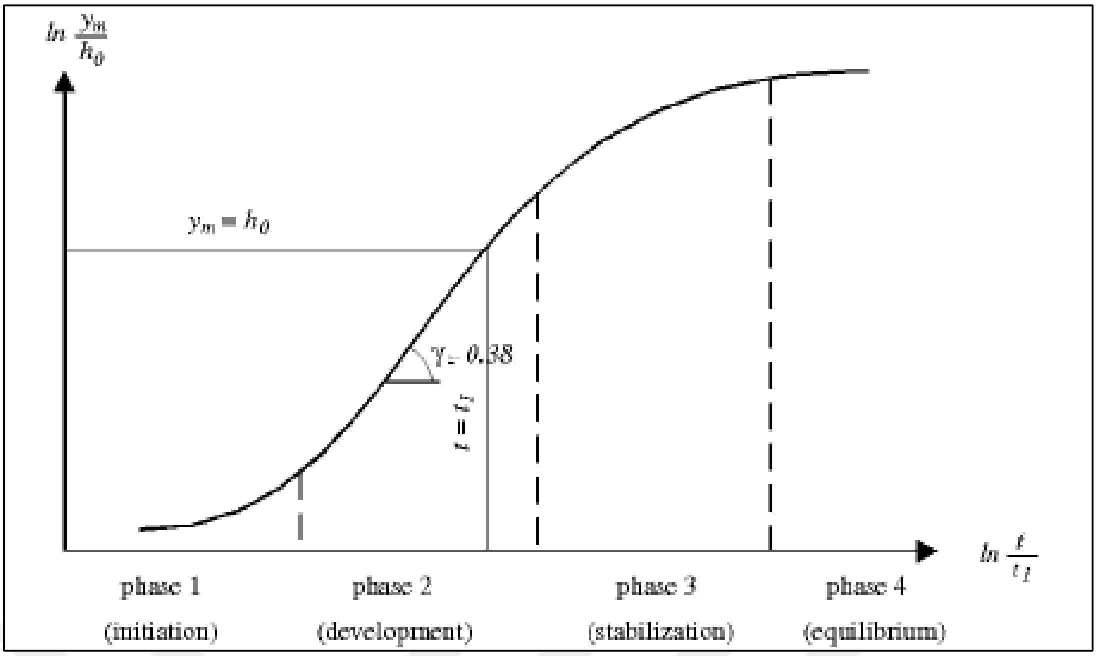

Figure 2.6 Development of scour process (Hoffmans and Pilarczyk, 1995)

2.5 Mechanism of Sediment Transport in Open Channel

Sediment particle is transported and deposited in another place. Erosion of particles is done by drag forces between the particles and adjacent water or air and gravity force. Properties of the bed materials and flow conditions are specified the mechanism of sediment transport. In the design of the hydraulic structure, the prediction of the scouring process is the important point.

Shields (1936) initial bed grain instability, which the problem using these parameters: the mean particle size, the fluid density, the kinematic viscosity, the sediment density and the bed shear-stress. The two main modes of sand transport are bed-load transport and suspended load transport as described below:

2.5.1 Bed load transport

The bed-load transport is defined to involve of rolling, sliding and saltating of particles in close contact with the bed is controlled by gravity forces acting on the particles and flow-induced drag forces. The bed load transport has three different modes of motion and verified by the bed shear velocity when the value of the bed-shear velocity just exceeds the critical value for motion, the particles will be rolling or sliding or both of them together. When increasing values of the bed-shear velocity, the particles will be moving along the bed by a regular jump, which is called saltation, the bed load layer is comprised of the fluidized sediment particles and fluid.

Bagnold (1956) defines the bed-load transport as that in which the successive contacts of the particles with the bed are strictly limited by the effect of gravity. Einstein (1950) defines the bed-load transport as the transport of sediment particles in a thin layer of 2 particle diameters just above the bed by sliding, rolling and sometimes by making jumps with a longitudinal distance of a few particle diameters.

2.5.2 Suspended load transport

This type of transport is the irregular motion of the particles through the water column induced by turbulence-induced drag forces on the particles detailed information is presented by Van Rijn (1993). The suspended load transport can be determined by the depth-integration of the product of sand concentration and fluid velocity from the top of the bed-load layer to the water surface. While the suspended-load transport is defined as that in which the excess weight of the particles is supported by random successions of upward impulses imported by turbulent eddies.

When the value of the bed-shear velocity exceeds the fall velocity of the particles, the sediment particles can be lifted to a level at which the upward turbulent forces will be higher than the submerged weight of the particles and as a result, the particles may go into suspension due to turbulent velocity fluctuations. The particle velocity in the longitudinal direction is almost equal to the fluid velocity.

2.6 Numerical Studies

Sedimentation is the result of complex natural processes, including entertainment, transportation, soil separation and sedimentation. Not only are the three-dimensional flow and sediment transport equations nonlinear, unknowns are more than the available equations. It causes closure problems necessary for turbulence modeling. On the other hand, solution development is very difficult in generalized three-dimensional cases where both sediment and fluid flow are non-uniform and unsteady. Along with the rapid development of computers, numerical simulation has become an effective research tool. Also, CFD in recent years by researchers has been widely used.

In earlier work, because of the high three-dimensional nature of the problem, it should be treated with a three-dimensional model, but the numerical simulation is started from the two-dimensional simulation for practical reasons. According to Morales and Ettema (2012), the 2D model provides ideas for several limited parameters, these models are based on a reduction in the amount of cell size compared to the 3D Model, and it is indicating a practical advantage. Morales and Ettema (2012) compared the experimental data with two-dimensional simulation output in the compound channel. The obtained numerical value was investigated and a strong correlation with the experimental data was observed.

Despite some of its advantages, the 2D model could not answer many questions arising due to the scouring of the hydraulic structural problem. The two-dimensional model requires less processing resources than the three-dimensional model. The early 3D numerical problems with the flow in the open channel were done by Prinos (1990), Naot et al. (1993), Pezzinga (1994) ,Krishnappan and Lau (1986), mainly investigating uniform flow over compound channels.

The outcome is also the first CFD commercial model with the ability to model the local scouring of complex structures without typical limits of structured boundary fitting grids is available from Flow-3D software. A good agreement with measurements described in the literature observed from the results showing that for complex structures the Flow-3D software is a powerful hydraulic design tool.

2.7 Numerical Model

2.7.1 Governing equations

The governing equations of flow are the momentum equation and the continuity equation :

$$\frac{\partial \mathrm{u}_i}{\partial x_i} = 0, \qquad (2.1)$$

$$\frac{\partial \mathrm{u}_i}{\partial t} + u_j \frac{\partial \mathrm{u}_i}{\partial x_j} = -\frac{1}{\rho}\frac{\partial \mathrm{P}}{\partial x_j} + \frac{\partial}{\partial x_j}\left(2vS_{ij} - \overline{u_i' u_j'}\right), \qquad (2.2)$$

$$S_{ij} = \frac{1}{2}\left(\frac{\partial \mathrm{u}_i}{\partial x_j} + \frac{\partial \mathrm{u}_j}{\partial x_i}\right), \qquad (2.3)$$

$$\overline{u_i'u_j'} = v_t\left(\frac{\partial \mathrm{u}_i}{\partial x_j} + \frac{\partial \mathrm{u}_j}{\partial x_i}\right) - \frac{2}{3}k\delta_{ij}. \quad (2.4)$$

Where u_i' is the fluctuation of fluid velocity in i direction, u_i is the fluid velocity component in i direction, P is the pressure, $\overline{u_i'u_j'}$ is the Reynolds stress tensor, ρ is the fluid density, v_t is the turbulence viscosity, $S_{ij}$is the mean strain rate tensor, v is the fluid kinetic viscosity, k is the turbulent kinetic energy, and $\delta_{ij}$is the Kronecker delta (δ_{ij} =1, *i=j;* $\delta_{ij} = 0$,*i=j).*

2.7.2 Turbulent model equations

Yakhot and Orszag (1986) proposed an improved k - ε turbulence model named RNG (renormalization group) k - ε model whose coefficient cannot be obtained from experimental data, but the theoretical analysis. The RNG k-ε model has better adapted than the standard k-ε model. For simulating the SB flow field and scour process RNG k-ε model was used in this study. In Flow-3D the governing equations are (1) 3D Reynolds-averaged Navier-Stokes equations for Boussinesq approximation with fluid flow, (2) the continuity equation and (3) the transport equation.

(k-ε) model flow was to provide a reasonable approximation for many kinds of flow, additional transport equations for turbulent diffusion are solved, εT:

$$\frac{\partial \varepsilon_T}{\partial t} + \frac{1}{V_F}\left(uA_x\frac{\partial \varepsilon T}{\partial x} + vA_yR\frac{\partial \varepsilon T}{\partial y} + wA_z\frac{\partial \varepsilon T}{\partial z}\right) = \frac{CDIS1.\varepsilon T}{k_T}\left(P_{T+CDIS3.G_T}\right) + DIff\varepsilon - CDIS2\frac{\varepsilon_T^2}{k_T} \quad (2.5)$$

$$\frac{\partial \mathrm{k}}{\partial t} + u_j\frac{\partial k}{\partial x_j} = \tau_{ij}\frac{\partial \mathrm{u}_i}{\partial x_j} + \frac{\partial}{\partial x_j}\left[\frac{1}{\rho}\left(\mu + \frac{\mu_t}{\sigma_k}\right)\frac{\sigma_k}{\partial x_j}\right] - \varepsilon \quad (2.6)$$

$$\frac{\partial \varepsilon}{\partial t} + u_j\frac{\partial \varepsilon}{\partial x_i} = C_{1\varepsilon}\frac{\varepsilon}{k}\tau_{ij}\frac{\partial \mathrm{u}_i}{\partial x_j} + \frac{\partial}{\partial x_j}\left[\frac{1}{\rho}\left(\mu + \frac{\mu_t}{\sigma_k}\right)\frac{\partial \varepsilon}{\partial x_i}\right] - C_{2\varepsilon}\rho\frac{\varepsilon^2}{k} \quad (2.7)$$

Here CDIS1, CDIS2, and CDIS3 are all dimensions user-adjustable parameters and have defaults of 1.44, 1.92 and 0.2, respectively for the (k−ε) model.

The diffusion of dissipation, Diffε is:

$$\text{Diff}\varepsilon = \frac{1}{V_F}\left\{\frac{\partial}{\partial x}\left(v\varepsilon A_x \frac{\partial_{\varepsilon T}}{\partial x}\right) + R\frac{\partial}{\partial y}\left(v\varepsilon A_y R \frac{\partial_{\varepsilon T}}{\partial y}\right) + \frac{\partial}{\partial z}\left(v\varepsilon A_z \frac{\partial \varepsilon_T}{\partial z}\right) + \xi \frac{v\varepsilon A_{X\varepsilon_T}}{x}\right\} \quad (2.8)$$

The rate of turbulent energy dissipation, $\varepsilon_{T,}$ the one-equation model is related to the turbulent kinetic energy K_T

$$\varepsilon_T = CNU \sqrt{\frac{3}{2}\frac{k_T^{3/2}}{TLEN}} \quad (2.9)$$

Where CNU is a parameter (0.09 by default), K_T is the turbulent kinetic energy and TLEN is the turbulent length scale.

In below equation where k is the turbulent kinetic energy, $k = \frac{1}{2}\overline{u_i' u_j'}$.

$$\tau_{ij} = \frac{\mu_t}{\rho}\left(\frac{\partial u_i}{\partial x_j} + \frac{\partial u_j}{\partial x_i}\right) - \frac{2}{3}k\delta_{ij} = C\mu = 0.085, C_{1\varepsilon} = 1.42, C_{2\varepsilon} = 1.68, \quad (2.10)$$

$$\sigma_k = 0.7179, \qquad \sigma_\varepsilon = 0.7179$$

Dissipation of turbulent kinetic energy, $\varepsilon = v\ \overline{\left(\frac{\partial u_i'}{\partial x_k}\right)\left(\frac{\partial u_i'}{\partial x_k}\right)}$; μ_t is the turbulent eddy viscosity, $\mu = C\mu\rho k^2/\varepsilon$; τ_{ij} is the Reynolds stress.

2.8 Sediment Transport Model in FLOW-3D

The scour model in Flow-3D can predict the motion of the packed and suspended sediment, which applies to the erosion near the hydraulic structures. The model has two important modules, lifting and drifting, as defined by Brethour J. (2003). Lifting model roles as the lift force created by the shear stress to separate the materials from the sediment bed. Drifting models produce the driving force on the sediment particle to be suspended in the flow, which is called the drift-flux model. The sediment behavior is controlled by the drag model. When the sediment concentration exceeds a cohesive soil fractions, it behaves as the solid and the drag model is activated.

In Flow-3D, the spreading of sediments in the flow field comprises of the packed and suspended sediment particles are advection and drifting, packed sediment particles can transport only if they become suspended when drag and lifting models initialed particles. When a suspended sediment increases it is caused to increase in fluid viscosity, after reaching the sediment or solid concentration to the cohesive solid fraction, it will not have any influence on the alteration of the fluid viscosity. At that state, the sediment behaves like a solid, which is reflected by the interaction among particles. An additional linear drag term in the momentum equation predicts the solid-like behavior (Flow-3D User Manual).

CHAPTER 3

CASE-STUDY

3.1 General

This study is based on the experimental study of Tiwari et. al., (2014) to simulate a 3D CFD model of the scouring phenomena in the SB and the effect of the intermediate sill on the quantity of scouring. The experiment was done in the hydraulics laboratory at Department of Civil Engineering, M.A.N.I.T. Bhopal, Madhya Pradesh India. This experimental test was simulated by Flow-3D software to getting the good aspect for scouring in the SB with a different type of sills.

3.2 Setting up of Physical Model and its Procedure

From the previous research, the physical modeling tests were done in the Hydraulic Laboratory of M.A.N.I.T., located in Bhopal, Madhya Pradesh India, that USBR type VI SB with end sill and impact wall was used. The study was performed in a flume of 58.8 cm wide 1 m deep and 25 m long with the ratio of the width to the equivalent diameter of noncircular outlet equal to 6.3 as per the limitation of (Gardes et al., 1986). A rectangular pipe with dimensions 10.8 cm. x 6.3 cm. was used to signify the outlet flow. The outlet of the pipe was put above SB bed by (1d =9.3cm). In the SB the impact wall was made with size 20.46 cm.x58.8 cm with the 9.3cmx58.8cm hood and end sill that equal height and base (1d). In order to investigate the scour at the end of the SB, the layer of the coarse sand applied that passed through the IS sieve of 2.36 mm and retained on 1.18 mm with height 9.3 cm, width 58.8 cm and the test section about 1.5 m.

The discharge was observed by a calibrated ventilator installed in the supply tube. In this work, four different types of intermediate sill were used as shown in Figure 3.1 to 3.5 for pipe Froude number (3.85) that's equivalent to a discharge of 19. 8 l/s. To observe the effect of pipe Froude number model-1 and mode-2 tested with two other different Froude numbers (1.85 and 2.85) that are equivalent to a discharge 9.5 l/s and 14.7 l/s respectively. In this section, the geometric designs and hydraulic of all five models that used for experimental and numerical modeling are explained. The maximum depth of scour was measured.

The models consist of pipe outlet, one impact wall and the SB with intermediate and end sills, as shown in the following:

Model-1

In the model-1 it has not intermediate sill, but one sloping end sill is located at the start of the erodible area. As shown in Figure 3.1.

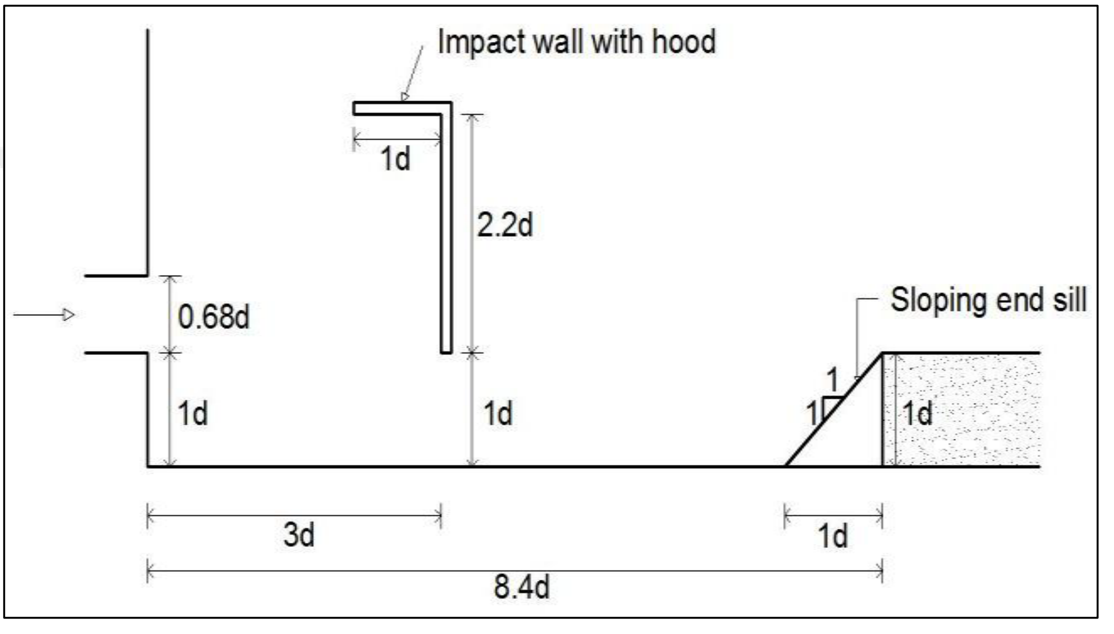

Figure 3.1 USBR type VI stilling basin without intermediate sill

Model -2

In the model-2 there is a triangular intermediate sill with equal base and height and vertical face downstream, also a sloping end sill. As shown in Figure 3.2.

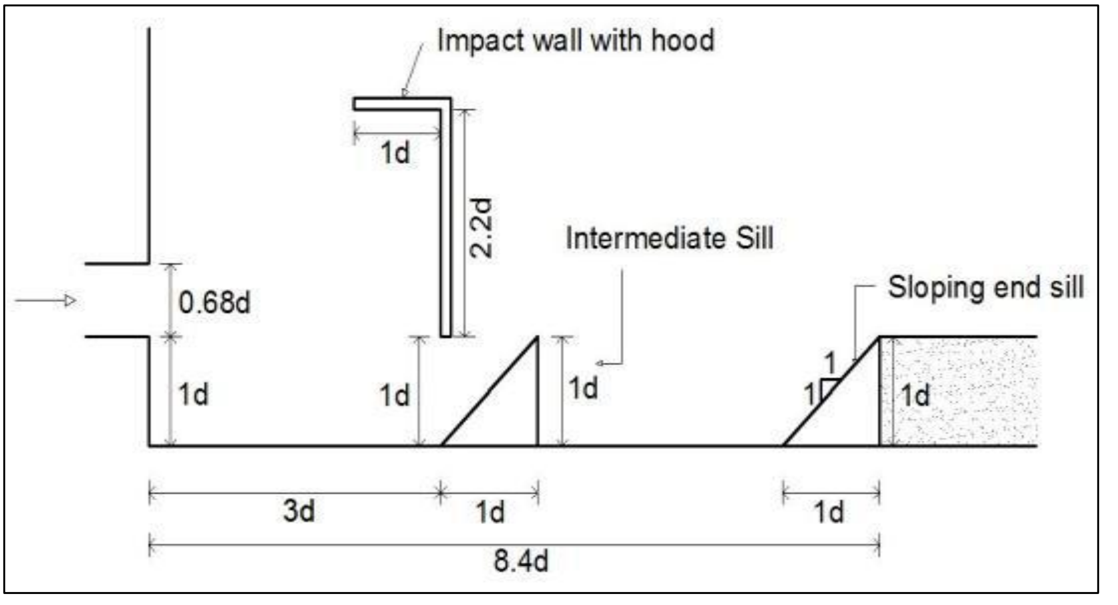

Figure 3.2 USBR type VI stilling basin with triangular intermediate sill that equal base and height

Model-3

In the model-3 there is a triangular intermediate sill with a base equal half height and vertical face downstream, also a sloping end sill just before the erodible area. As shown in Figure 3.3.

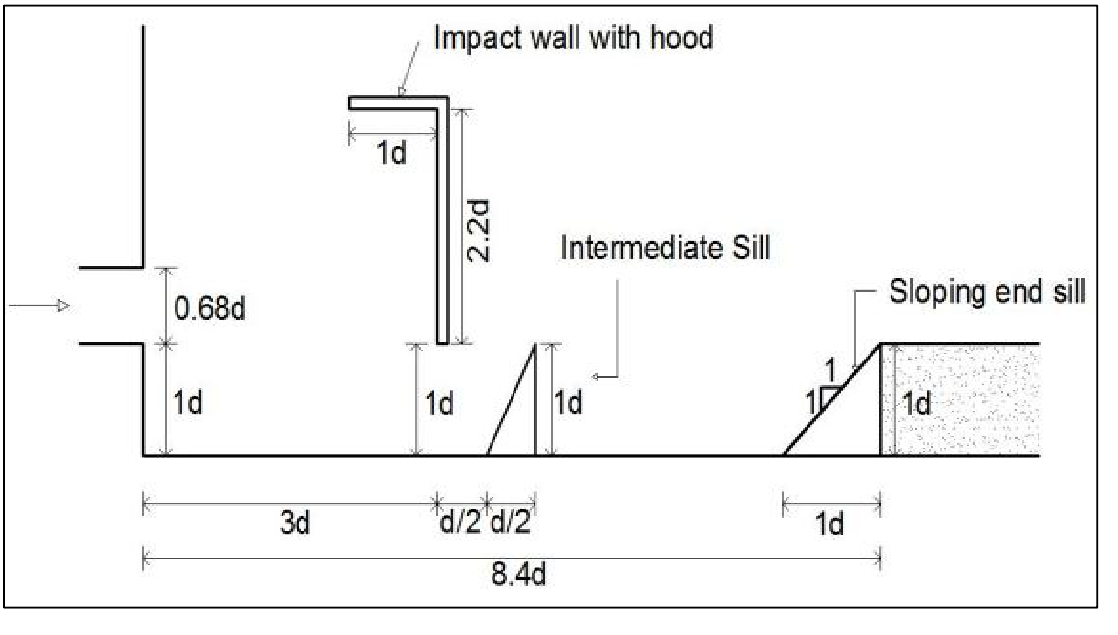

Figure 3.3 USBR type VI stilling basin with intermediate sill of a base equal half height

Model-4

In the model-4 there is a rectangular intermediate sill with a base equal 0.2 height and a sloping end sill just before the erodible area. As shown in Figure 3.4.

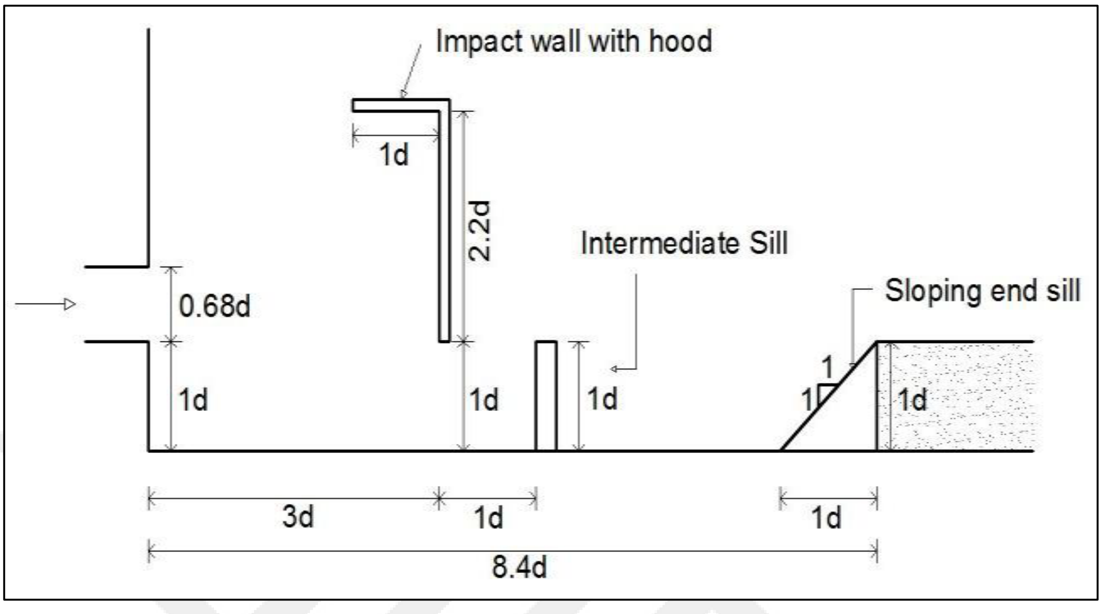

Figure 3.4 USBR type VI with rectangular intermediate sill

Model-5

In the model-5 there is a square intermediate sill with equal base and height and a sloping end sill just before the erodible area. As shown in Figure 3.5.

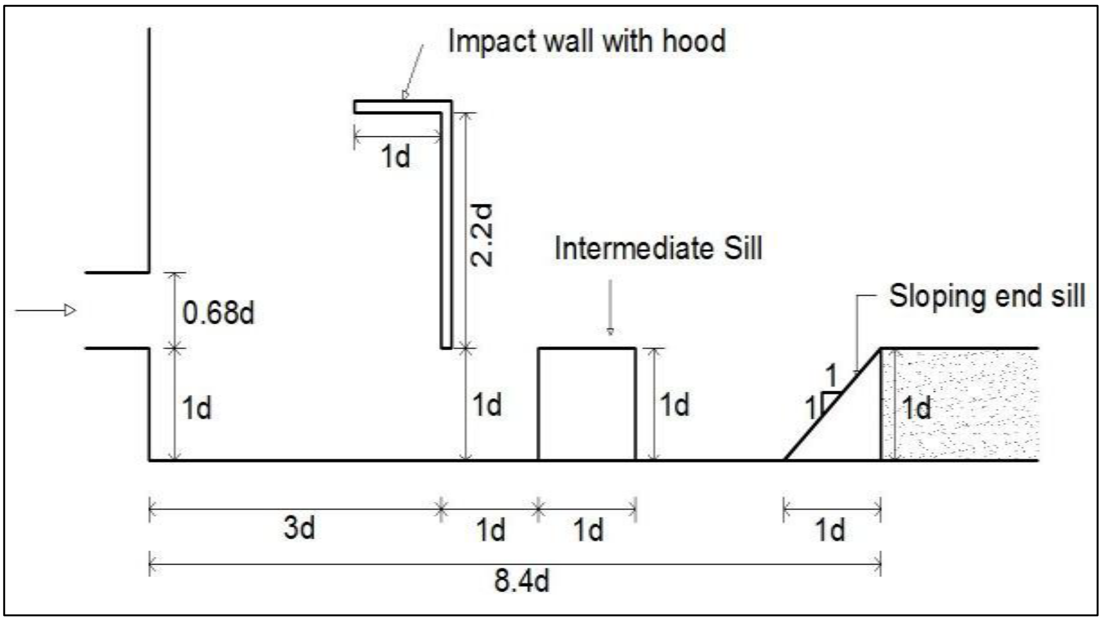

Figure 3.5 USBR type VI stilling basin with square intermediate sill

USBR type VI SB model has been tested with impact wall and end sill and for other four models were tested with four different geometry intermediate sills. All tests were carried out with the same erodible material for all models. The dimensions of impact wall and intermediate sill shown in Table 3.1.

Table 3.1 Geometry of the stilling basin

Testing of Models to study the intermediate sill geometry with triangular end sill (1V:1H) of height 1d for basin length 8.4d								
S.N.	Model Name	USBR VI Impact Wall with hood			Intermediate sill			
		Size	Bottom gap with basin floor	Location from out let exit	Shape	Height	Width	Location from out let exit
1	Model-1	1d×2.2d	1d	3d	—	—	—	—
2	Model-2	1d×2.2d	1d	3d	Triangular with vert ical face D/S	1d	1d	4d
3	Model-3	1d×2.2d	1d	3d	Triangular with vert ical face D/S	1d	d/2	4d
4	Model-4	1d×2.2d	1d	3d	Rectangular	1d	0.2d	4d
5	Model-5	1d×2.2d	1d	3d	Square	1d	1d	4d

3.3 Numerical Model Steps

This work was simulated based on experiments conducted by Tiwari et. Al., (2014) with a slight difference by adding an apron 2cm after the end sill, because of the Flow-3D solution depends on the grid mesh and the end sill is triangular, top thickness very small and program it cannot read a small object, thereby the program cuts the top part and it doesn't represent the actual case to solve this problem the apron was added and on the other hand the sand depth was increased to 20cm.

Generally, CFD procedure has three major steps, the first step is pre-processor, second one solver and last is post-processor. In any software, the pre-processing is the data inputting to performing the solver step and the solver is computing the model with the parameters that inputted in the previous step and the post-processor in output the required data and rearranging.

Numerical simulation beginning with a computational grid. In the pre-processor the computing field is represented by the number of interconnected components also, the grid generation is describing the shape and the simulating field of the problem.

Grid generation is an important step in the CFD simulations because of the accuracy of the simulation mainly depends on it. In the preprocessing stage introduce the properties of a fluid by boundary condition and initial condition.

The computed field discretizes forms flowing fluid and solve governing equations at the solver step. The flow parameters are calculated in any computational cell.

In post processor phase, there is a lot amount of data on the simulated model, the Flow-3D advanced by means of visualization and post processing tools for evaluating this results and obtaining the summary and required data in the shape of the two dimensional and three dimensional surfaces, vector, contour plots, flow lines, grid display text data output ISO surfaces, geometry, and a lot of graphs could be drawn. Furthermore, it is included animation tools for exhibiting dynamic results. Figure 3.6 shows the step of CFD analysis.

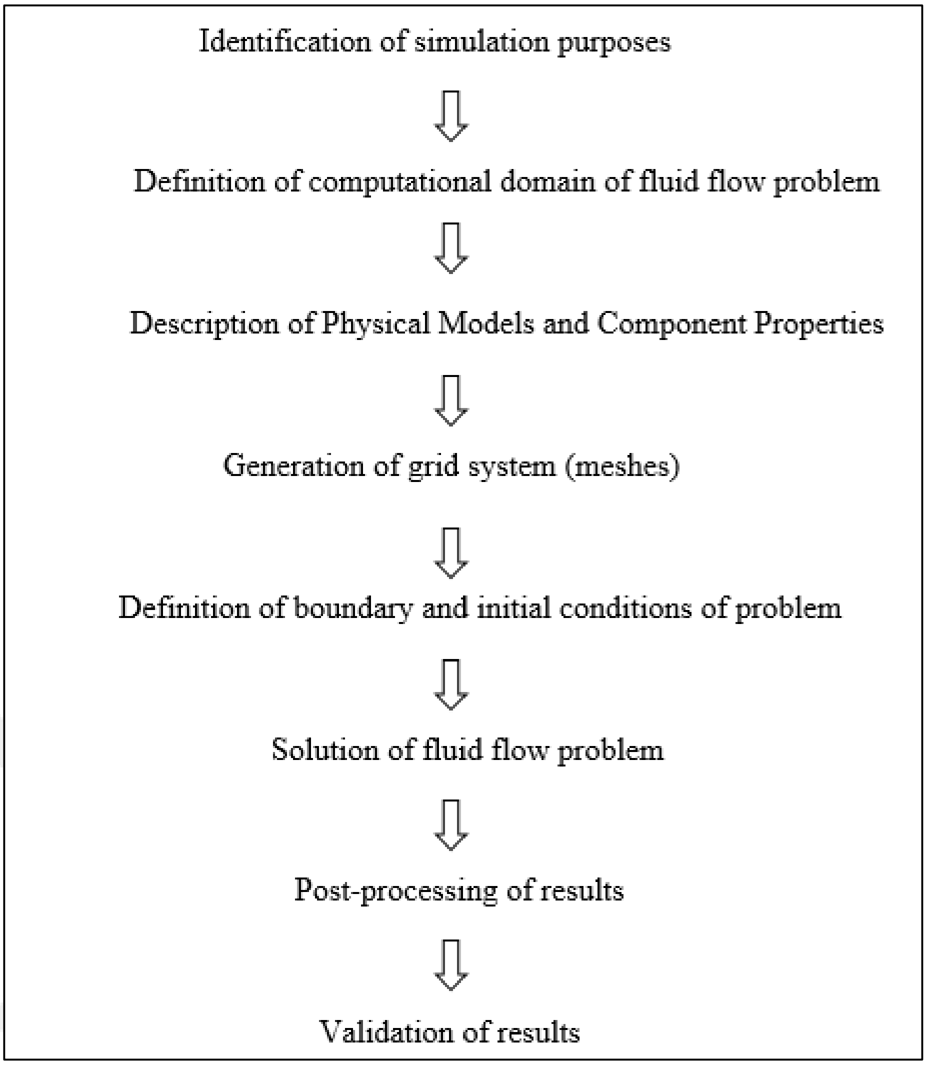

Figure 3.6 Steps in CFD analysis

3.4 Brief Introduction to Flow-3D

Flow-3D software is a powerful software and commercial packages that used to analyze numerical models, which are developed by Flow Science Inc. (Flow Science, 2008). The software puts on some exceptional features to the numerical solution of the continuity equations and Navier-Stokes equations are discretized and solved in each computational cell, for Open Channel Flow (VOF) and meshing of compound geometries (FAVOR) method is used.

In this study, Flow-3D software was used in the solver step. It is a capable tool for complex flow and sediment scour modeling. Flow-3D is simulating problems with high accuracy and it applying of TruVOF for the surface flows. Flow-3D can solve the Navier-Stokes in 3D to simulate the continuity equations with the fluid flow equations for the turbulence magnitudes. To solve the RANS equation, the program uses a finite volume method. A mesh, which is a rectangular cell grid is formed by dividing the simulating domain.

After dividing the computational area into rectangular grids, the solution is obtained on each cell. The simulating cells are recognized in x-direction (i), y-direction (j) and z-direction (k). At the center of the cell the quantity of the scalar is calculated while on the face of cells tensors and vector are calculated. as shown in Figure 3.7.

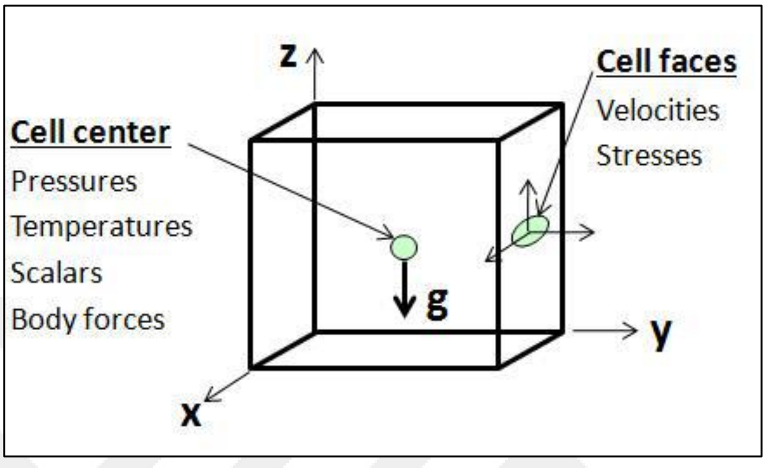

Figure 3.7 Grid system (Flow-3D proposed by hydraulic training, 2012)

In this software there are many selections for numerical simulation that are added or improved to the basic Navier-Stokes equations. These items describe the turbulence effects, sediment leaching, moving solids, fluidization, granular flows, solid state deformation, porous media, heat transfer, cavitation, air entrainment and surface tension.

3.5 VOF and FAVORO Methods

VOF and FAVORO are illustrations of volume-fraction methods. In these two ways at first the area is subdivided into a control volume grid or a small element. For elements containing liquid each parameters of flow such as temperature, pressure values and velocity within the element are calculated, usually these values represent some sort of volumetric average of the quantities in the element.

3.5.1 VOF method

The surface of the fluid that is divided in to regular cells, all cells in the top are not fully contained fluid, but some of the cells are partially full and some of these elements are filled with fluid, on the other hand partially filled elements are called free surface that is filled with air and liquid.

A suitable way to identify the state of cells is to find the F quantity that represents the fraction of the cell volume filled with liquid, this amount is called Volume of Fluid (VOF). In the CFD the interface between the gas pressure and the liquid is called free surface. A free surface is generally a good approximation between liquid density and gas density that have a high difference.

In recent years, several methods have been used to approximate free boundaries in finite difference numerical simulation. A simple and powerful method that is explained based on the concept of a fractional volume of fluid (VOF). This method has been shown to be more flexible and more efficient than other methods dealing with complex free boundary configurations.

The free surface of Flow-3D is modeled using fluid volume (VOF) technology, which was first informed in (Nichols and Hirt,1975). The VOF method consists of three ingredients such as scheme to locate the surface, an algorithm to track the surface as a sharp interface moving through a computational grid and a means of applying boundary conditions at the surface.

Fluid configurations are defined in terms of a volume of fluid (VOF) function, F (x, y, z, t) (Hirt-Nichols, 1981).

$$\frac{\partial F}{\partial t} + \frac{1}{V_F}[\frac{\partial}{\partial x}(FA_{xu}) + R\frac{\partial}{\partial y}\left(FA_{yv}\right) + \frac{\partial}{\partial_z}(FA_{zw}) + \xi\frac{FA_{xu}}{x} = F_{DIF}+F_{SOR} \tag{3.1}$$

$$F_{DIF} = \frac{1}{V_F}\{\frac{\partial}{\partial x}\left(v_F A_x\ \frac{\partial F}{\partial x}\right) + R\frac{\partial}{\partial x}\left(v_F A_y R\frac{\partial F}{\partial y}\right) + \frac{\partial}{\partial_z}\left(v_F A_z\frac{\partial F}{\partial z}\right) + \xi\frac{v_F A_{xF}}{x} \tag{3.2}$$

$$V_F\frac{\partial \rho}{\partial t} + \frac{\partial}{\partial x}(\rho u A_x) + R\frac{\partial}{\partial_y}\left(\rho_v A_y\right) + \frac{\partial}{\partial_z}(\rho_w A_z) + \xi\frac{\rho_u A_x}{x} = R_{DIF} + R_{SOR} \tag{3.3}$$

Where V_F is the fractional volume open to flow, ρ is the fluid density, R_{DIF} is a turbulent diffusion term, and R_{SOR} is a mass source. The velocity components (u, v, w) are in the coordinate directions (x, y, z) or (r, R_{SOR}, z). A_x is the fractional area open to flow in the x-direction, A_y and A_z are similar area fractions for flow in the y and z directions, respectively. The coefficient R depends on the choice of coordinate system.

3.5.2 FAVOR method

The FAVORO technique is another fractional volume method, used only in define the geometry. This fractional volume of liquid method may be used to define the solid surface so that the fractional volume of the liquid of each element of the grid is used to position the fluid surface. Indeed the volume fraction (V f) of the element which is not blocked by the solid. It has proven advantageous to store blank parts on each side of the element. In any case, regardless of whether you are storing an open or blocked part of an element, you can use the same technique used in the VOF method to identify the solid boundary to cut the fixed grid. This information is used to define the boundary conditions of the wall to which the flow must conform.

Since the geometry of the flow limit is generally stationary, the volume fraction Vf and the surface fraction Af need not be moved or changed with the flow. While the VOF technique is shared with the FAVORO technique, the amount of liquid F is defined as the fraction Vf of the open volume of the element, and not the proportion of the total volume of the element. In other words, if G is the volume of the element, the actual liquid volume of the element is (FVf) G instead of (F) G.

3.6 Numerical Model Setup

The numerical model was simulated with Flow-3D (2012) by using RNG k-ε model. The maximum scour has been calculated for five models of SB. The program simulates the fully three dimensional transient Navier-Stokes equations using the VOF and FAVOR method. To discretize the computational domain, the solver uses finite volume approximation. In each case, one fluid has been used that is a water at 20 degrees Celsius for all simulations.

3.6.1 Physics

The Flow-3D software has many physical options, for scouring modeling, there is four specified parameter needs to be taken to obtain accurate results on scouring and flow field. The gravity option was activated in the downward vertical gravitational acceleration being set to negative 9.81 m/s^2 as shown in Figure 3.8.

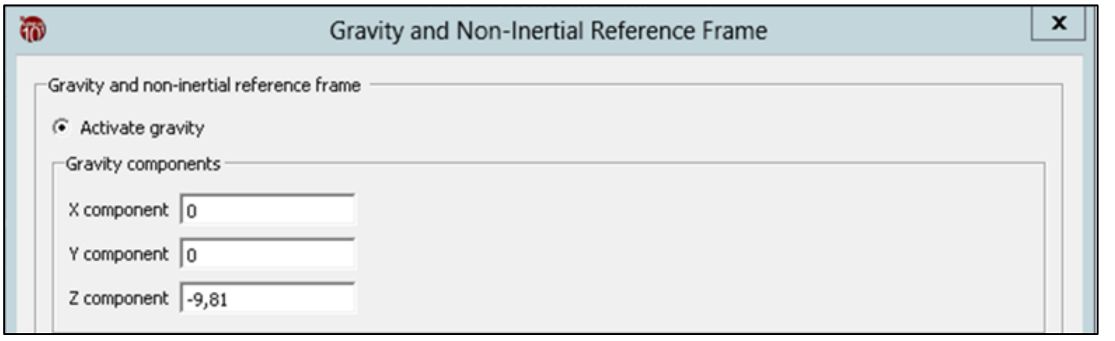

Figure 3.8 Gravity component

As illustrated in the Figure 3.9 viscosity and turbulence options were also activated. Each option includes a different alternative, there are five different elections in turbulence option, for this study RNG model has been selected.

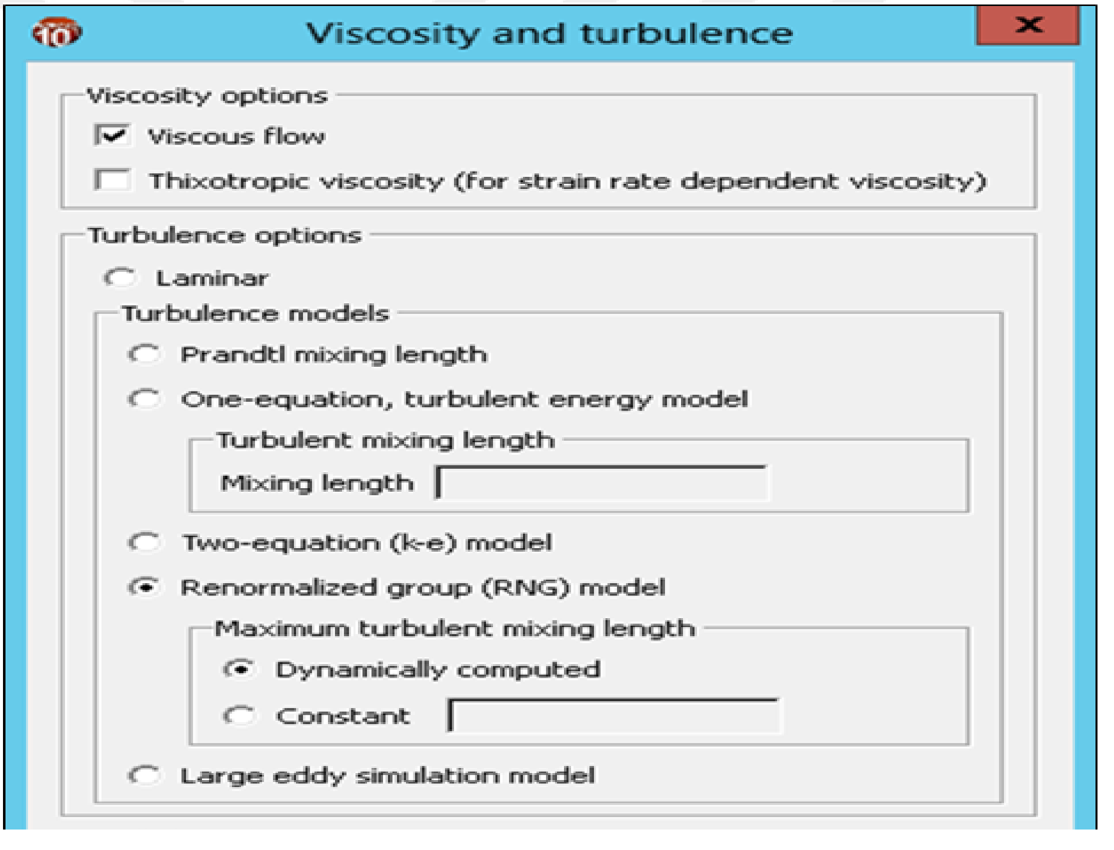

Figure 3.9 Viscosity and turbulent option

The sediment scour model is activated in the user interface and the parameters of the sediment particles are inputting to the window as shown in Figure 3.10.

- The number of sediment particles, in this study one type of particle was used.
- The maximum packing fraction the default value is 0.64.

- The Richardson-Zaki coefficient multiplier The default value of the program is 1.0
- The species diameter is the mean particle diameter(d_{50}) is equal to 1.77 mm.
- The density of the sediment particles in (kg/m^3) is equal to 2650.
- The critical shields number, FLOW-3D from the Shields curve will calculate the number.
- The drag coefficient equal to 1.5 this value is appropriate for sand and gravel (Engelund and Hansen, 1967).
- The entrainment coefficient which, controls the rate at which particle erodes at a shear stress higher than the critical shear stress, the default value is 0.018 from (Mastbergen and VandenBerg, 2003).
- The bed Load coefficient, which controls the rate of the bed load transport, the used value of this study is 8.0. The researchers suggested that the values ranging from 5.0 for low transport to 13.0 for very high transport.
- The Angle of Repose is the maximum resting angle of the bed materials typically between 30 and 40 degrees in this study 35 degrees were used.

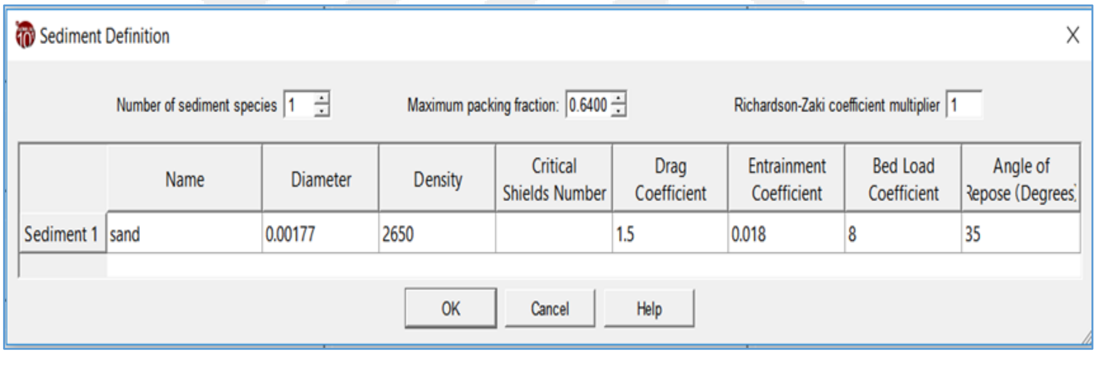

Figure 3.10 Scour parameters

Another physical option that activated in the scouring simulation is the density evaluation as shown in Figure 3.11.

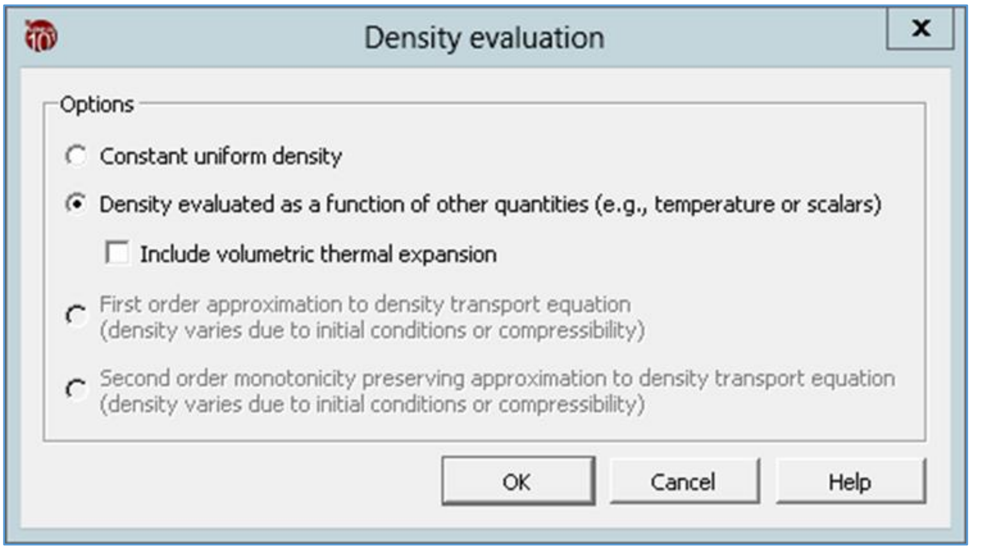

Figure 3.11 Density evaluation

3.6.2 Turbulence model solvers

In the FLOW-3D software has five turbulence simulation model for computing the turbulent flow and scouring process. These are; Prandtl's mixing length model, one-equation (k) model, two-equation (k-ε) model, Renormalized group (RNG k-ε) model and Large Eddy Simulation (LES) model in this study RNG model was used to simulate scour model because of RNG k-ε model it can accurately solve flow field with turbulence and high shear stress (FLOW 3-D User Manual, 2013).

(Zhaoding Xie, 2011) studied that the different turbulence models for simulation of scouring he found that the results of RNG model more accurate than other models when compared with the literature study from experimental investigations.

3.6.3 Geometry

For obtaining accurate data in Flow-3D, it is necessary to be designed precise geometry model fit the physical model and imported to the Flow-3D. The simple model can be created by Flow-3D, but the complex model it can use the Auto-Cad, solid work software or any software that has (stl) format. The geometry of the SB for each model was modeled in Auto-Cad software and exported as a stereolithographic (stl) format. The stl file was directly imported into the Flow-3D, but the original coordinates point should be known in Auto-Cad or other software to creating the meshes fit to the model. See Figure 3.12.

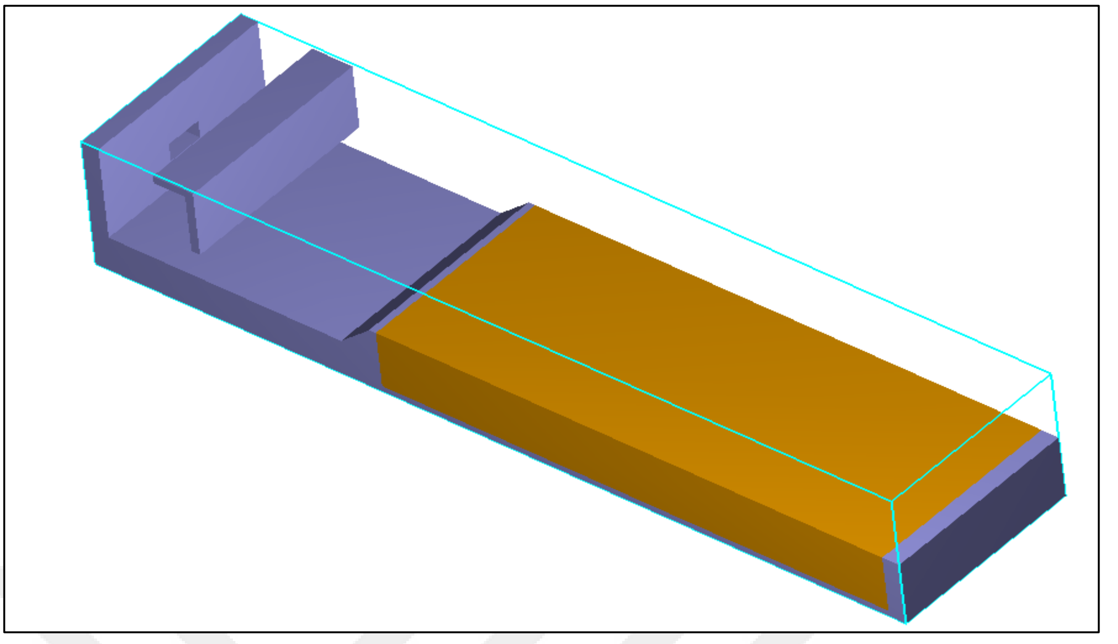

Figure 3.12 Stilling basin geometry in Flow-3D

3.6.4 Meshing

A mesh is a subdivision of the flow and sediment particles domain and domain is discretized into a finite set of control volumes are called cells. Cell sizes in each block are very significant and it affects on the simulation time and the accuracy of the results in order to it is very important to use a suitable cell size that is valid to obtain a real result and reasonable computation time. In this study, the computational field sediment particle layer was divided into the cells and the mesh sizes in x,y, and z directions are 0.02 m.

3.6.5 Data sharing

FLOW-3D can generate output in the form of numerical data, images, and animations for sharing in presentations and embedding in reports. Figure 3.13 and 3.14 show the 3D and 2D computational domain, the models are 2.4 m long,0.588 m width and 0.45 m height, the mesh sizes in x,y and z directions are 0.02 m.

There are total number of cells (active and passive) = 98335 mesh cells in the simulation, and total number of active cells =74786 active cells include real cells used for solving flow equations

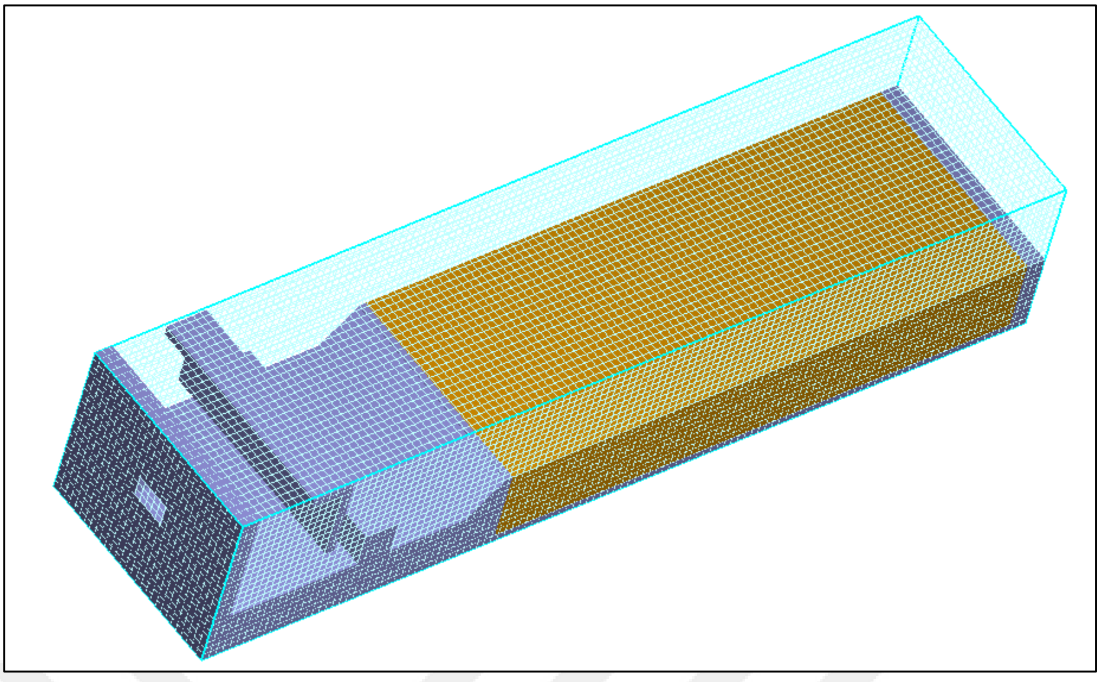

Figure 3.13 Representation of the geometry meshing of 3D model

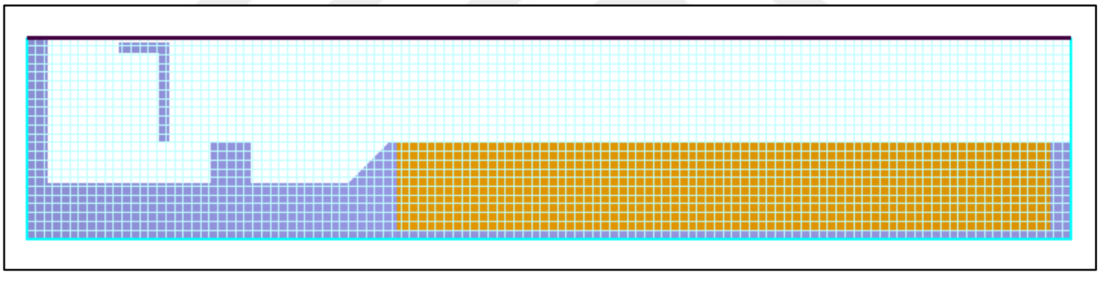

Figure 3.14 Representation of the geometry meshing of 2D model

3.6.6 Specifying boundary conditions

In the solving continuity equations and Navier-Stokes equations, suitable initial conditions must be selected. In Flow-3D software has ten different types of boundary condition for a specified state of the flowing fluid. The boundary conditions in Flow-3D are pressure, specific velocity, grid overlay, volume flow rate, wave, outflow, wall, periodic, symmetry, and continuative.

Figure 3.15 indicates the boundary conditions for the simulated SB model, as shown the upstream boundary (X min) is the volume flow rate (Discharge), the downstream (X max) is an outflow boundary while the bottom (Z min) is computed as wall boundary and the top (Z max) is specified pressure with zero fluid fraction, for both (Y min) and (Y max) were labeled as wall because to present the real situation of experimental.

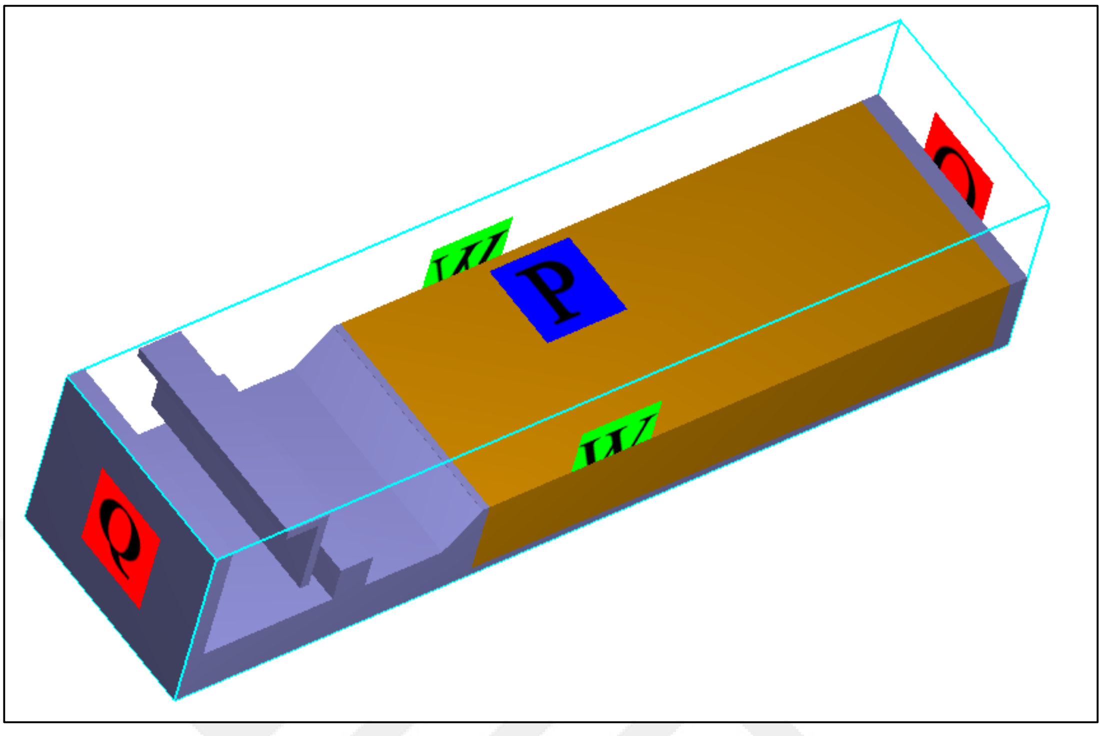

Figure 3.15 Boundary conditions

CHAPTER 4

RESULTS AND DISCUSSION

4.1 General

The results of maximum scour depth at the end of the SB have been found numerically by using Flow-3D software under clear water condition and compared with experimental results to assess the precision of the CFD program based on the experimental results from literature study. In this study, the USBR type VI stilling basin with impact wall and end sill were used and four different geometries intermediate sill were added to the SB to investigate the effect of the intermediate sill on the maximum scour depth and finding the best type of intermediate sill that reduces the scour depth to a minimum value.

Three different discharges for model-1 and model-2 were tested to observe the effect of water depth and flow rate on the scour depth at the end of the SB and compared with the experimental results. The effect of vorticity and Froude number on the scouring will be mentioned.

4.2 Comparison of Flow-3D and Laboratory Results

Table 4.1 shows the CFD and experimental results of maximum scour for all trials by changing sills geometry. The results showed that Flow-3D predicted the scour depth for most of the intermediate sills close to the laboratory results except model-5 that is a difference between numerical and experimental too high, in experimental work maximum scour depth for model-5 equal to 8 mm while the median size of sand equal to 1.77 mm, when compare this scour with the sand diameter the scour depth is unbelievable because it is very small. In the numerical results, the reduction in the scour depth by using intermediate sill was less than the reduction in the experimental results, in the experimental study difference between scour depth in model-1 and model-5 higher than the difference in the numerical results. However, the numerical results were not quite equal to the experimental, but it gives the similar conclusion to the best intermediate sill geometry.

Table 4.1 Numerical and experimental results

Models	Discharge l/s	Maximum scour depth (mm)	
		Numerical	Experimental
Model-1	9.5	43	32
Model-1	14.7	51	44
Model-1	19.8	59	46
Model-2	9.5	19	14
Model-2	14.7	30	24
Model-2	19.8	41	31
Model-3	19.8	52	43
Model-4	19.8	33	22
Model-5	19.8	27	8

The numerical investigation illustrated that the maximum depth of scour at the end of SB without intermediate sill was reduced by using intermediate sill, the effect of sill on maximum scour it depends on their geometry, for both numerical and experimental results the scour depth was reduced to minimum value by using the square intermediate sill Figure 4.1 shows the maximum scour depth for all models, to know the effect of sill geometry and finding the best type of sill that minimize scour depth to minimum value, SB was tested without sill and then four different sill geometry were added .

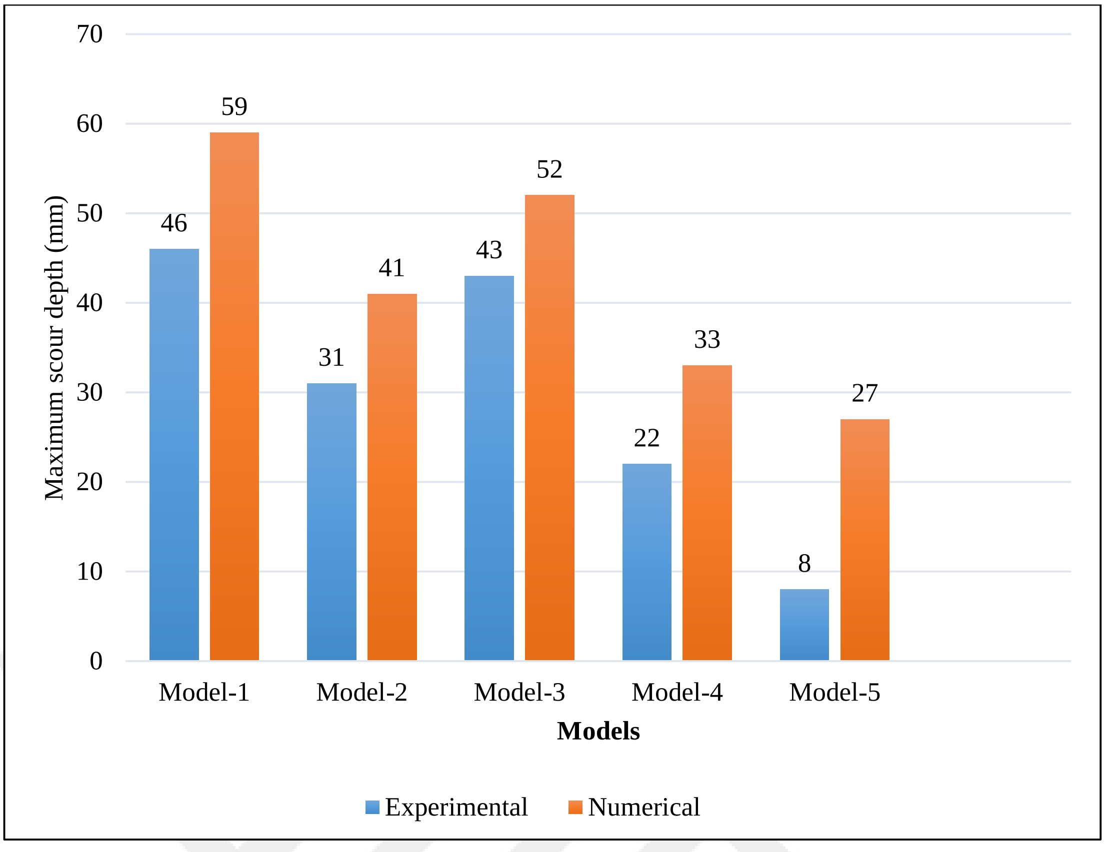

Figure 4.1 Experimental and numerical results for Q=19.8 l/s

The results showed that scour depth were reduced for all sill geometries and the best type of sill is square intermediate sill that reduced the scour depth to a minimum value. The local scour that took place at the end of the SB was due to the formation of vortex at the downstream phase of the end sill, the vorticity at the scour positions were increased and the flow rotation clearly appeared and the vortex shapes were changed for different sill geometry as illustrated in Figure 4.2 to 4.6, erosion of bed material near an obstruction that located in moving water it is caused by three dimensional turbulent flow near the structure. Wherever the turbulence intensity increase gives an increase in local transport capacity (Hoffmans and Pilarczyk, 1995). The flow pattern is accelerating around the obstruction in the result vortices is happened, the bed downflow impinging is the main cause of occurring the scour (Melville and Raudkivi 1977).

These below figures show the vortex vectors for each type of intermediate sill at the station 10 cm after the end sill and the scour depth reduced with reductions in the vortex vector. Kuhnle et. al. (2008) showed that the turbulence in the flow is lead to increase shear stress and then the erosive force capacity increases near hydraulic structure thereby the bed materials will be eroded.

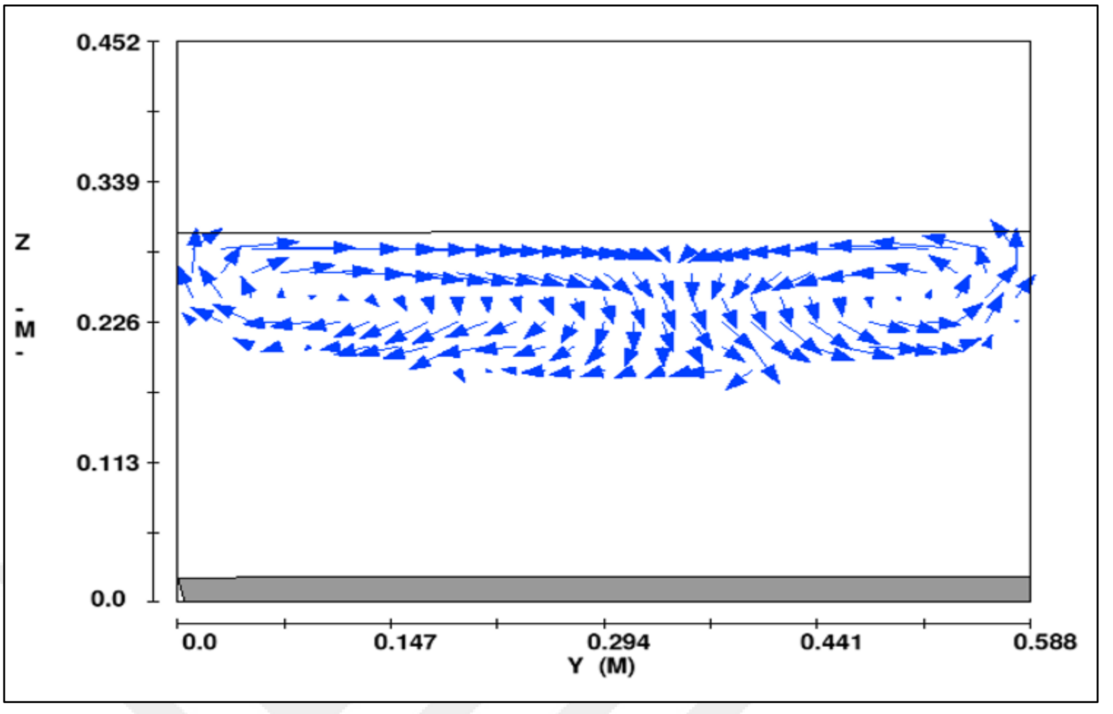

Figure 4.2 Vortex vector model-1 Q=19.8 l/s

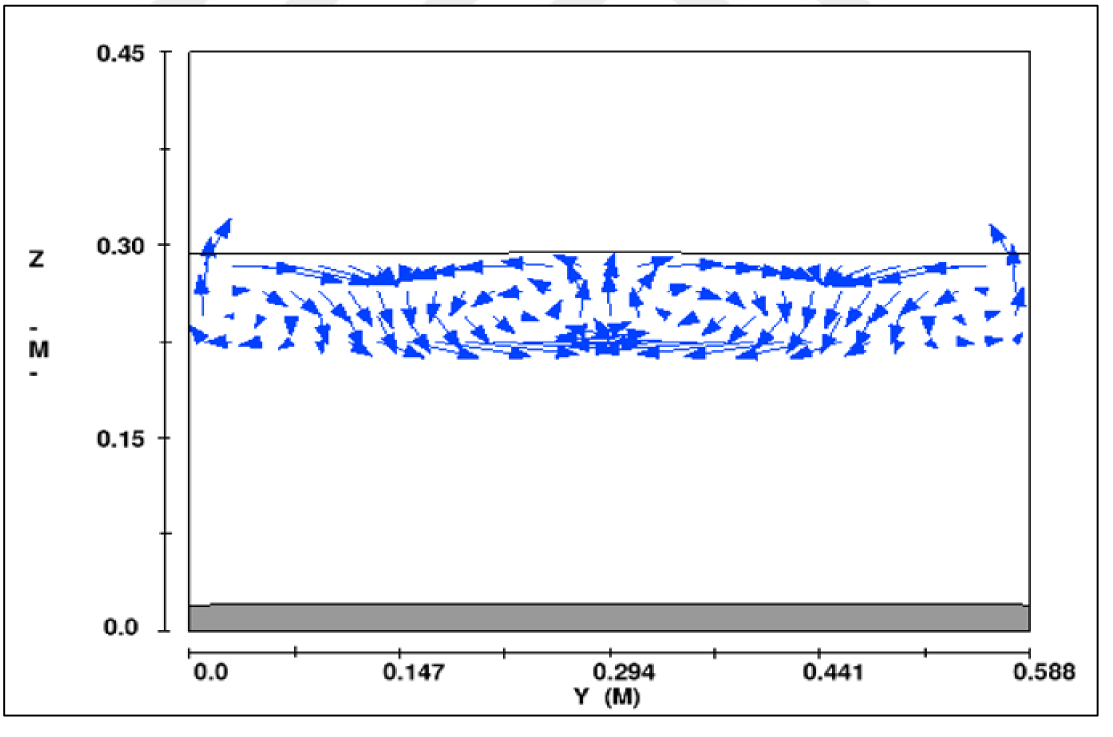

Figure 4.3 Vortex vector model-2 Q=19.8 l/s

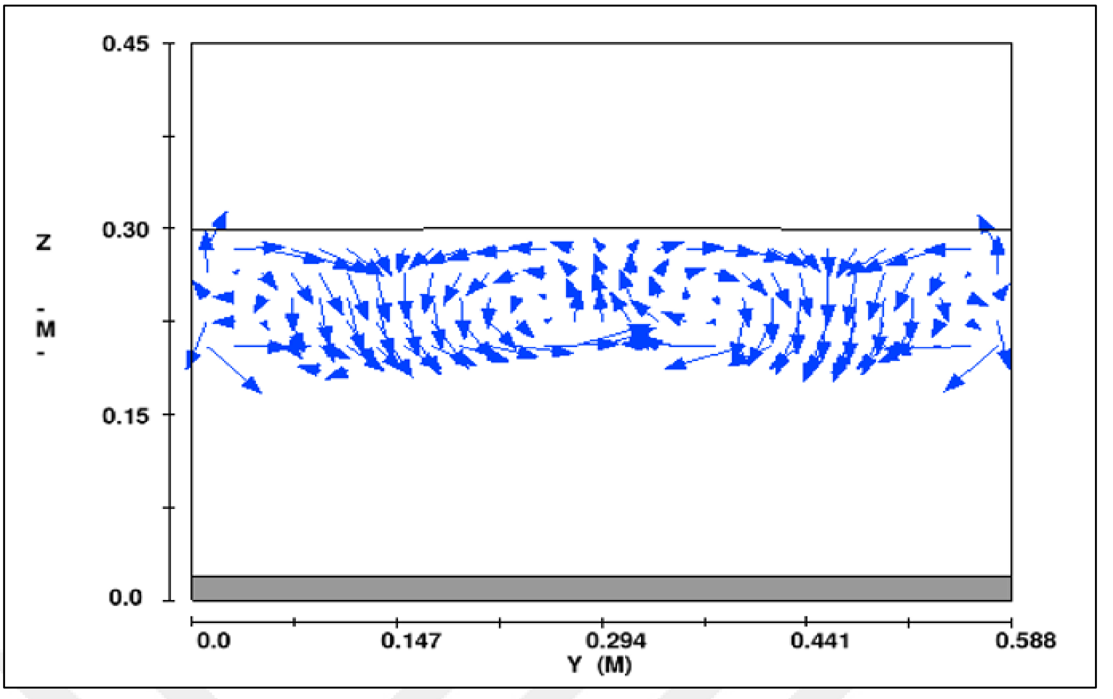

Figure 4.4 Vortex vector model-3 Q=19.8 l/s

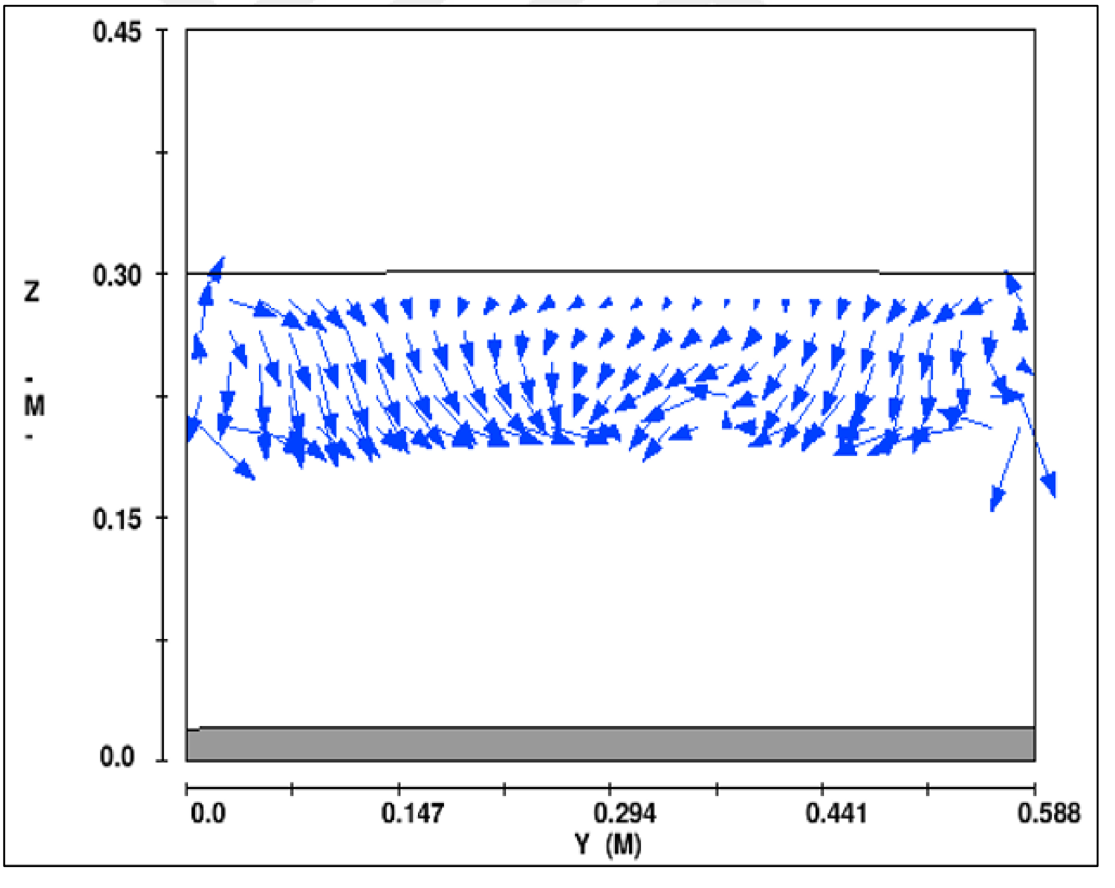

Figure 4.5 Vortex vector model-4 Q=19.8 l/s

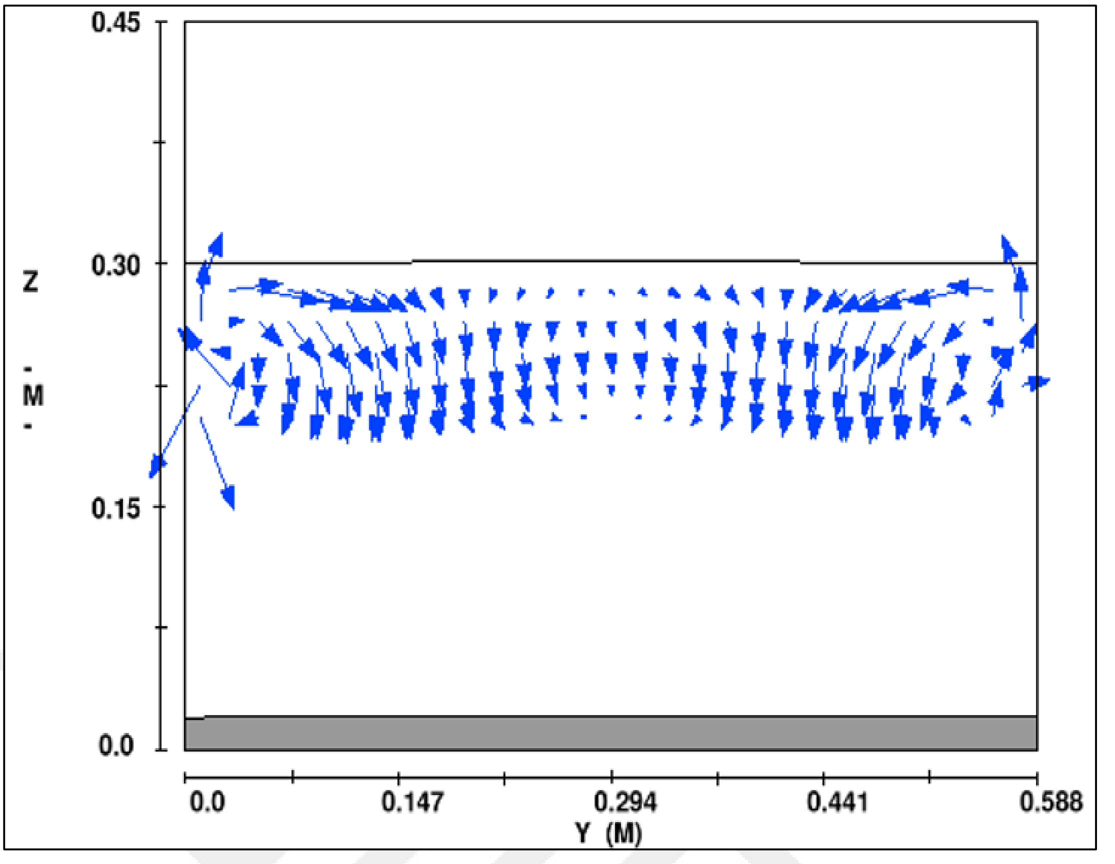

Figure 4.6 Vortex vector model-5 Q=19.8 l/s

It is essential to observe flow field and turbulence distribution around water control structures to investigate the local scour mechanisms and by investigating the turbulence property the local scour depth can be predicted and minimized by using scour protection such as appurtenances that used in the SB. When the bed shear stress exceeds the critical shear stress the bed material will be eroded and scour hole is starting formation. The figures above illustrate that have a strong relationship between vorticity and scour depth as showed the maximum scour in model-1 is equal to 59 mm but in model-5 is equal to 27 mm and vortex can be seen clearly that in model-1 is higher than model-5.

4.3 Centerline Profiles Along Horizontal Axis

Figure 4.7 to 4.11 illustrate the scouring profile along the channel at the downstream of the SB after the end sill through the centerline of the basin, for clear water scouring under a steady flow condition results for bed profile of basin without intermediate sill and by using different intermediate sill were shown. In both basin models with and without an intermediate sill, the scour hole goes to be the minimum value after a specified distance at the downstream of the end sill, and after this distance, the geometry of intermediate had not a great effect on scour hole.

As shown in the below figures the scour hole changes for each model in depth and forms. The maximum scour hole had formed in the SB model without an intermediate sill, while the scour hole geometry of this model is different from other models. Such geometry conditions are typically termed as a scour hole form, however the motion of objects that occurred in the scour hole associated with turbulence from vortex formation (Hopfinger et al., 2004; Gaudio and Marion, 2003).

Finally, it showed that the scour hole geometry proportionally changed with and without an intermediate sill. Flow turbulence and high bed shear stress around the structures initiate erosion and help the formation of scour hole, scour hole forms due to the combined effects of high bed shear stress and turbulence near the hydraulic structures (Chrisohoides et al. 2003).

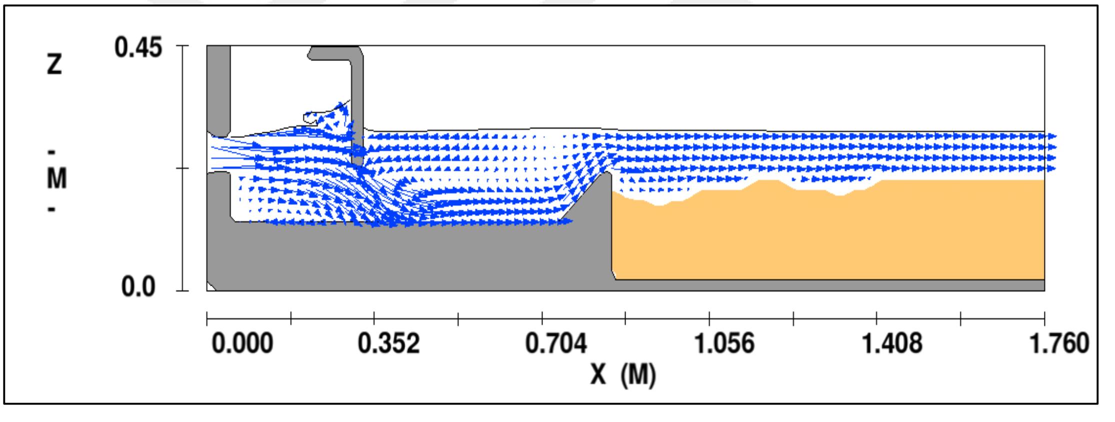

Figure 4.7 Scour profile at the centerline of basin for model-1 Q=19.8 l/s

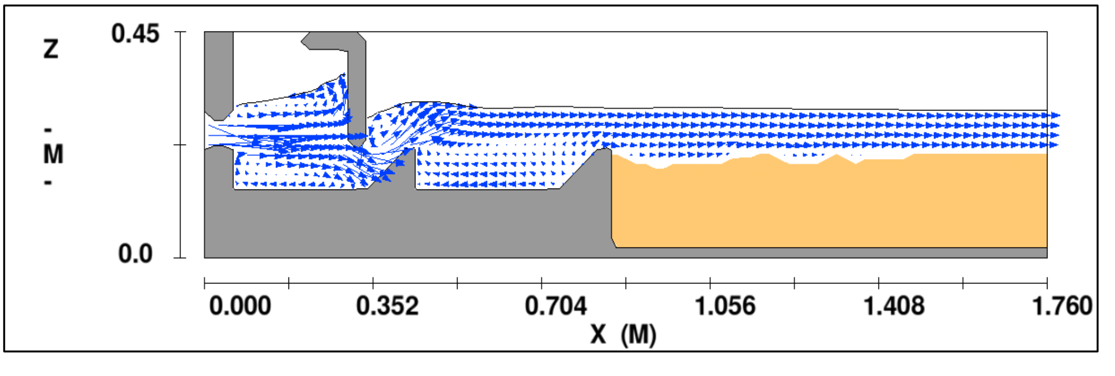

Figure 4.8 Scour profile at the centerline of basin for model-2 Q=19.8 l/s

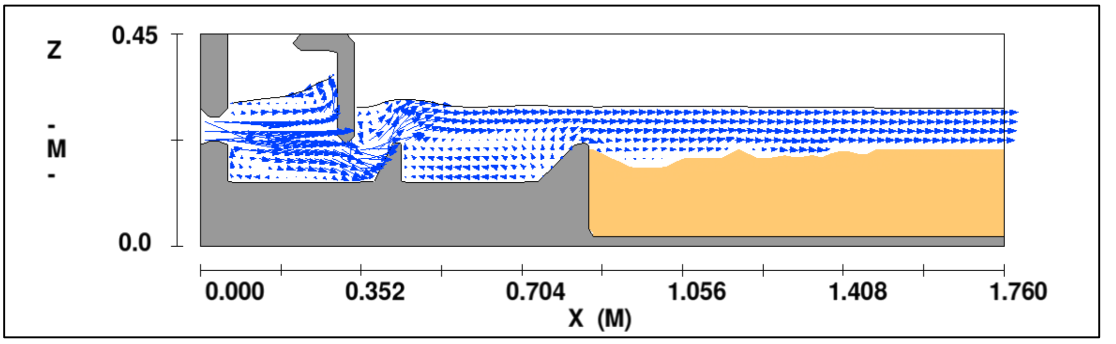

Figure 4.9 Scour profile at the centerline of basin for model-3 Q=19.8 l/s

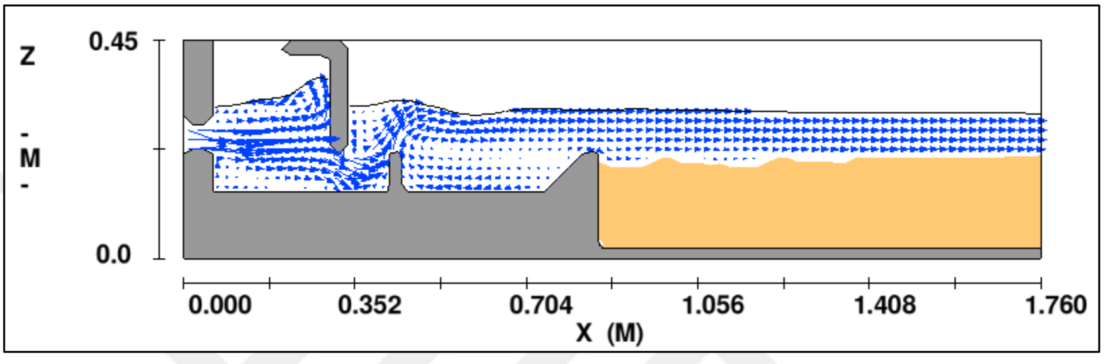

Figure 4.10 Scour profile at the centerline of basin for model-4 Q=19.8 l/s

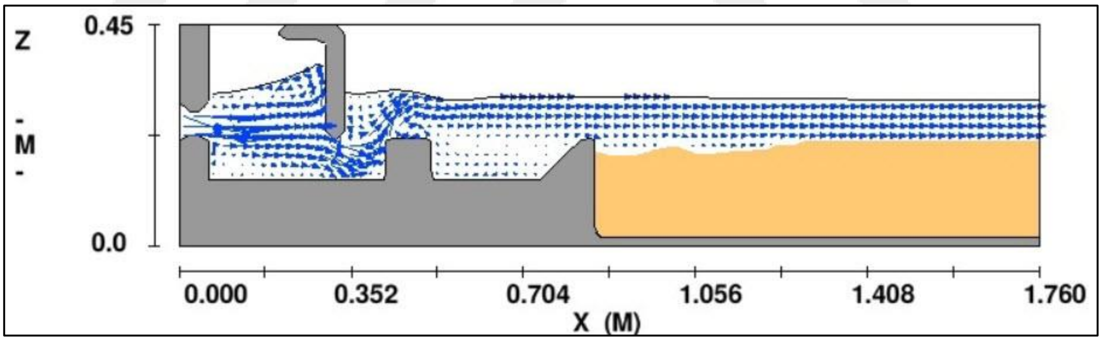

Figure 4.11 Scour profile at the centerline of basin for model-5 Q=19.8 l/s

From the centerline profiles can be observed as the scour depth increases in result development in the scour hole occurred from model-1 to model-5 as the scour depth increased the scour hole form were changed linearly, on the other hand as the distance from the stilling basin increased the scour depth decreased because of with increasing the distance from the water control structure the turbulent energy decreased thereby the scour depth will be reduced.

4.4 Transverse Scour Profile

The transverse profile of the scour depth across the position of maximum scour through the flume width illustrated in the Figure 4.12, it can see that the scour hole profile around the centerline of the channel is symmetric. The scour depth at the center of flume maximum and it goes to minimize on the channel sides, it could due to the velocity distribution along the width of the channel because of the cohesion between water and channel wall the velocity minimum at the channel sides and maximum at the center of the channel, on the other hand as presented in the figure may be due to the effect of vorticity that is located at the center of the channel.

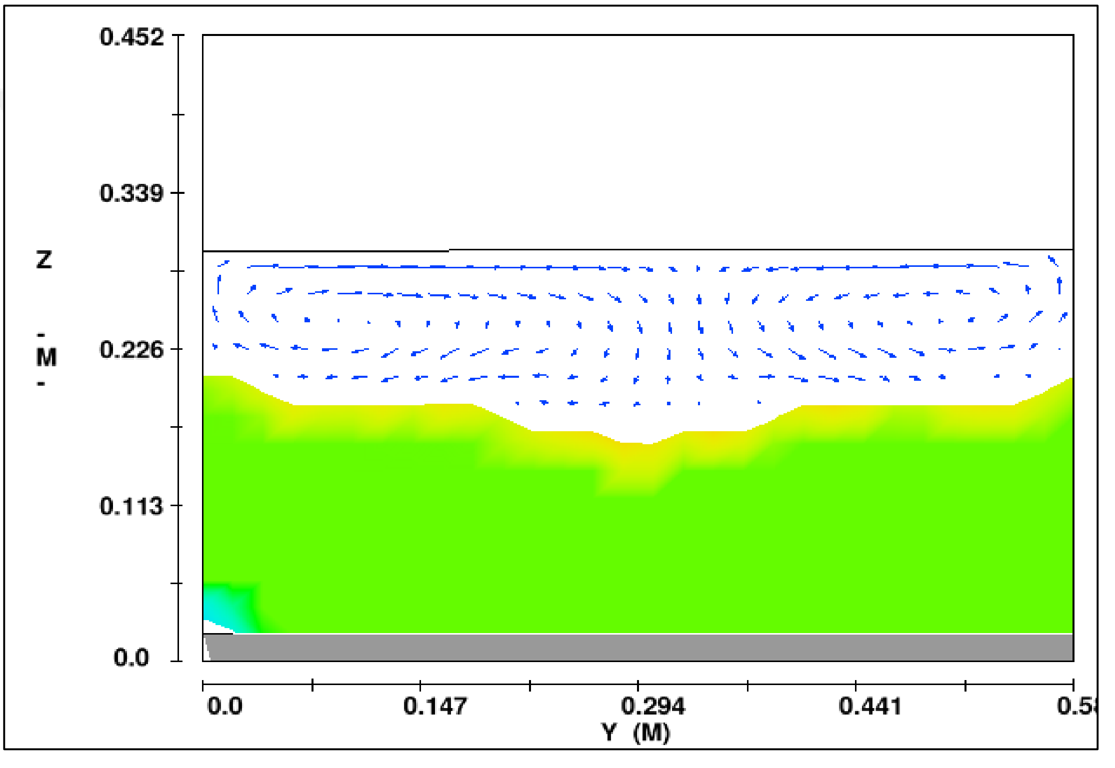

Figure 4.12 Transverse section of scour profile

4.5 Correlation of Scour Depth with Froude Number

Garde et. al. (1961) determined that the Froude number of open channel flow represents the effect of approaching flow on the maximum scour depth. Figure 4.13 to 4.15 shows the variation of Froude number and scour development for different discharges and results showed that an increase in the Froude number leads to increase in scour depth and scour hole development.

It has the linear relationship between scour depth and Froude number both flow depth and velocity effect on scour depth with an increasing in Froude number the scour depth was increased. The Froude number, $U/\sqrt{(gH)}$, shows the ratio of the inertial force to fluid gravitational force. A higher Froude number, means a larger resistance applied by water stream on the bed particles this is lead to more bed material will be eroded. Zaghloul (1983) included the flow Froude number in his analyses. As the flow rate increased the Froude number also increased as shown in the below figures for discharges of (9.5 l/s, 14.7 l/s and 19.8 l/s) respectively the indicated color for the specified position was changed and increases linearly with the discharge.

Whereas the depth of scour hole increases the Froude number tend to minimize as shown in the figures, in the place where the maximum scour depth the Froude number close to zero.

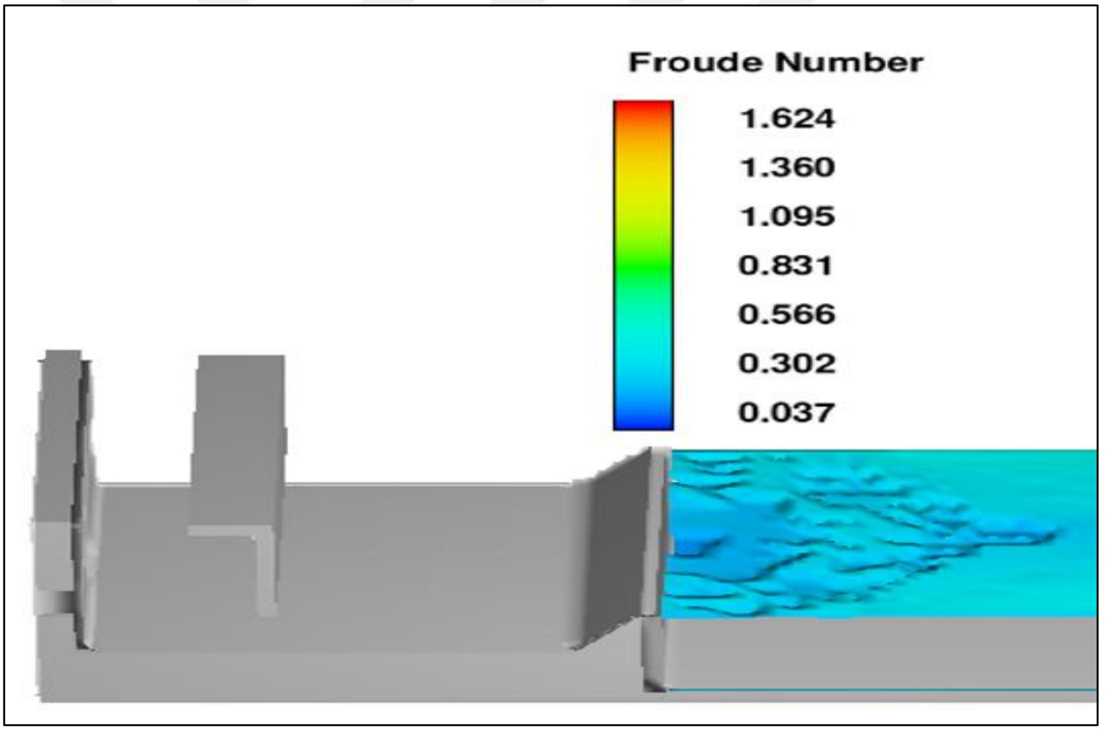

Figure 4.13 Correlation of scour depth with Froude number model-1 Q = 9.5 l/s

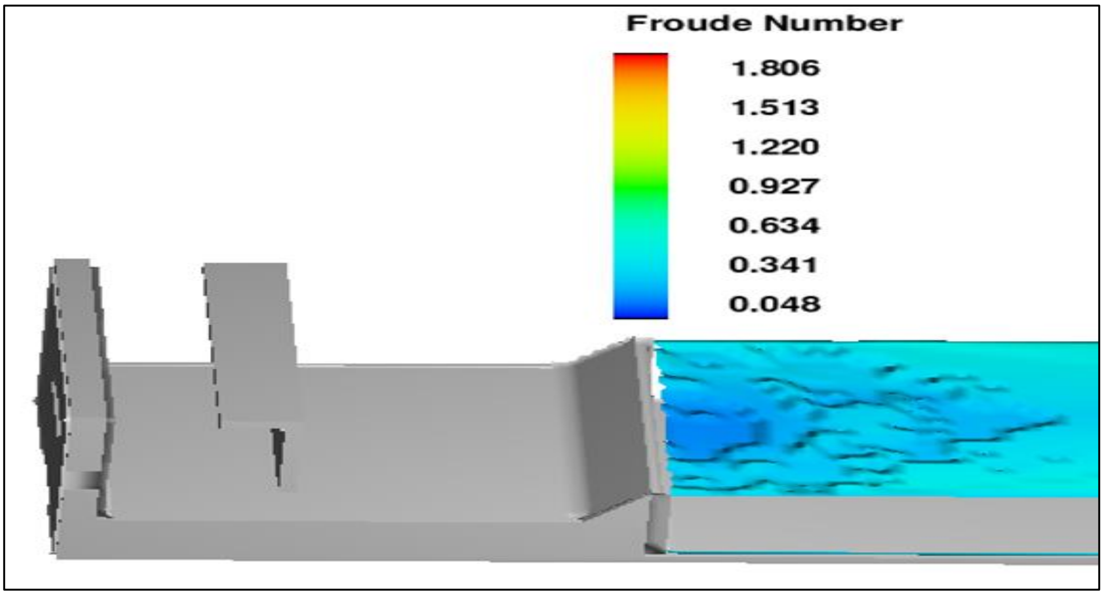

Figure 4.14 Correlation of scour depth with Froude number model-1 Q = 14.7 l/s

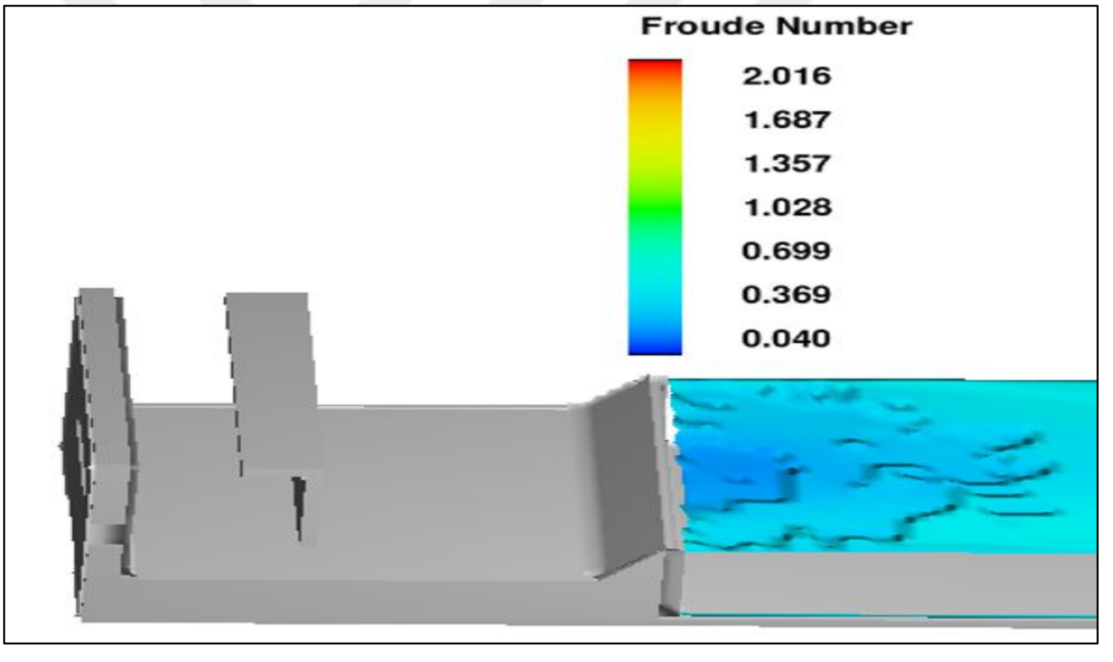

Figure 4.15 Correlation of scour depth with Froude number model-1 Q = 19.8 l/s

4.6 Effect of Discharge on Maximum Scour

Table 4.2 shows the results of maximum scour for three different discharges of (9.5 l/s, 14.7 l/s and 19.8 l/s) and their effects on the maximum scour depth, the results showed that by increasing flow rate the maximum scour depth was increased, it could be due to increasing flow velocity and bed shear stress. By increasing in flow rate the depth of flow increased, the maximum scour depth changes proportionally with discharge and flow depth because of the kinetic energy of the flow increases and destructive effect of the flow increases (Tareq, 2013).

Melville and Coleman (2000) conducted that in the conditions of clear water scour, the maximum scour depth increases linearly with velocity this means that by increasing discharge the velocity increased hence the maximum scour increased. By increasing discharge, the flow depth increased and this increase in flow depth it is lead to increase in maximum scour depth as shown in Figure 4.16 to 4.18. Laursen (1952) studied that the flow depth is an important factor to measure the scour depth and effects is proportional with scour depth.

Table 4.2 Scour depth for different discharge

Models	Discharge(l/s)	Scour depth (mm) Numerical	Scour depth (mm) Experimental
Model-1	9.5	43	32
Model-1	14.7	51	44
Model-1	19.8	59	46
Model-2	9.5	19	14
Model-2	14.7	30	24
Model-2	19.8	41	31

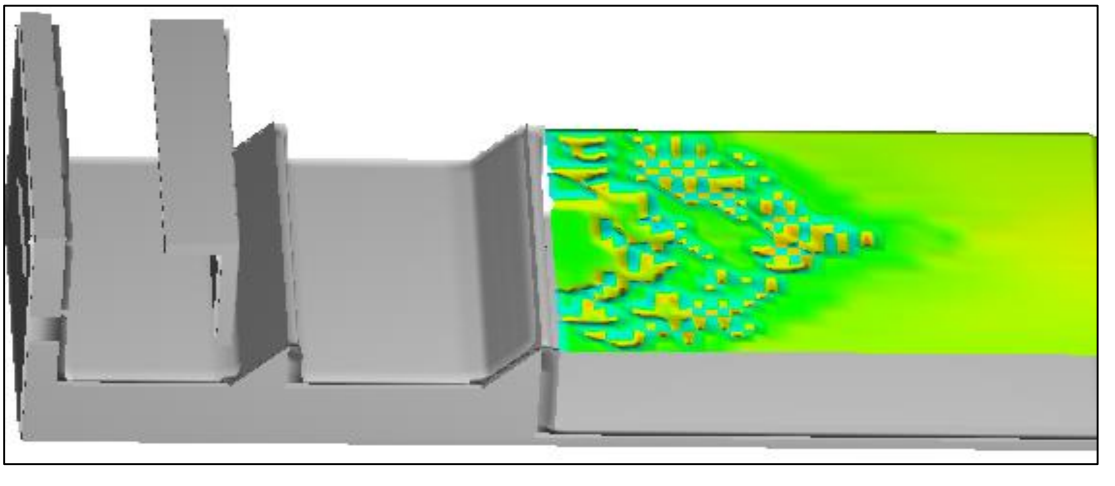

Figure 4.16 Scour hole geometry for model-2 Q = 9.5 l/s

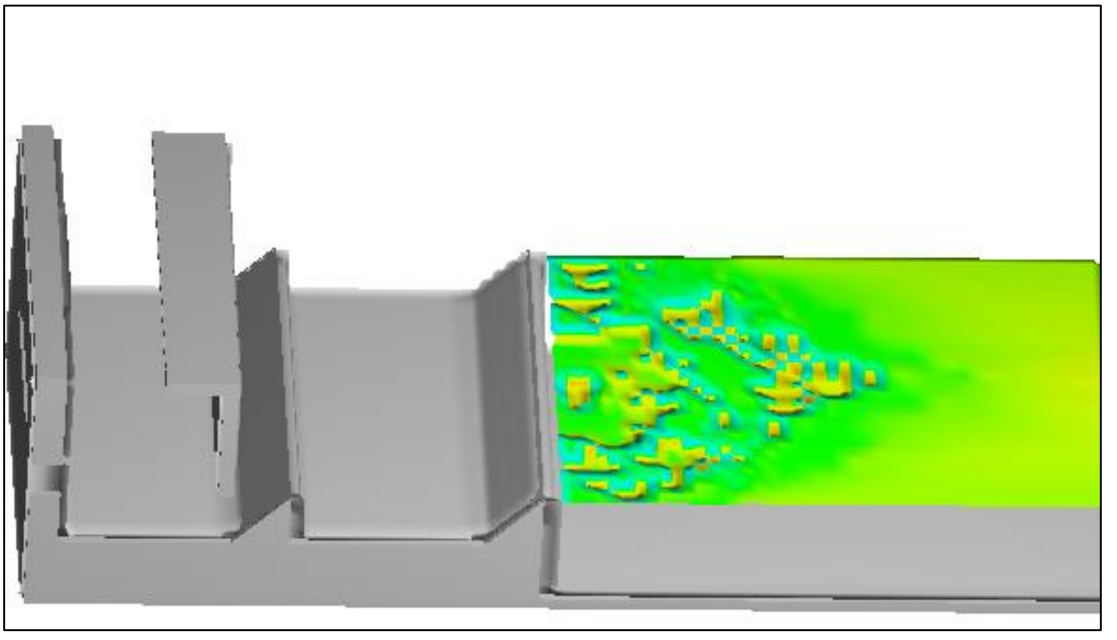

Figure 4.17 Scour hole geometry for model-2 Q =14.7 l/s

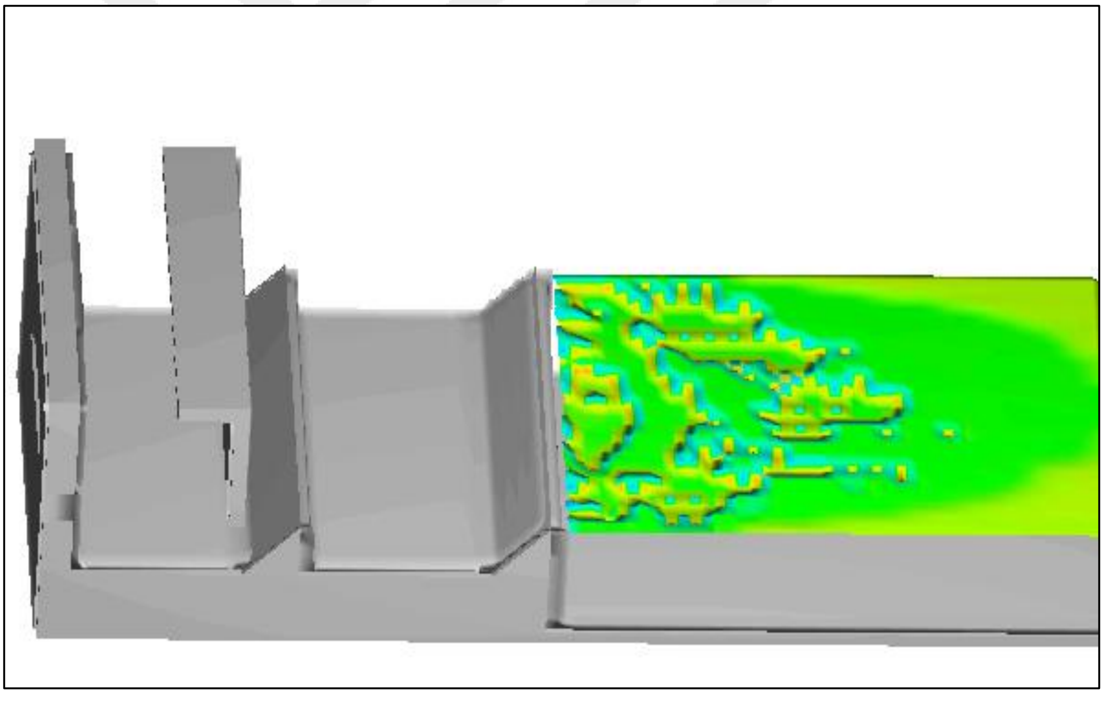

Figure 4.18 Scour hole geometry for model-2 Q = 19.8 l/s

CHAPTER 5

CONCLUSIONS AND RECOMMENDATIONS

5.1 Conclusion

The scope of this research to predict the phenomenon of scour at the downstream of the SB and to investigate the effect of intermediate sill on the maximum scour at the end of the SB with end sill and impact wall, in order to improved SB model for scouring reduction that is based not only on the CFD Modelling using for scour prediction but this study is verified by the experimental study from literature research. Additionally, the proposed SB model and different intermediate sill geometry used in the experimental study also found to have the same in this numerical investigation and the conclusions for the best type of intermediate sill are the same but only have a difference in the amount of scour reduction in experimental and numerical. The study has an important application in selecting a best SB geometry to reduce the depth of maximum scour at the end of water control structure. The results showed that the maximum scour depth depends on the SB geometry and it is appurtenances. Flow condition has a great effect on scour depth such as discharge, Froude number, turbulent energy and velocity.

The maximum scour at the end of the SB is significantly reduced by using intermediate sill and geometry of intermediate sill has an important role in minimizing scour depth, the results showed that the best type of intermediate sill that reduces the scour depth to the minimum value is the square intermediate sill and be considered as the best type of intermediate sill.

Important conclusions in this study are discussed below:

1-This study presents the good agreement between experiment and CFD results for scour depth and in evaluating of best sill geometry, for both experimental and numerical have the same conclusions about the best type of intermediate sill, but only the difference between CFD and experimental results for maximum scour in model-5 are too high.

2-The accuracy of the Flow-3D software has been confirmed by simulating existing laboratory study and comparing the CFD results with laboratory outcomes.

3-The Flow-3D results from this study when compared with the experimental results in both of them intermediate sill has a great effect on depth of scour at the end of the SB.

The effect of intermediate sill in reducing scouring at the end of the SB depends on sill geometry, the best type of intermediate sill that reduces the scouring to the minimum value is the square intermediate sill.

4-The scour depth at the end of the SB affected by some flow characteristics such as vorticity, Froude number and flow rate.

5-Flow-3D is a suitable tool to complement experimental investigation. But, extensive term simulations have to be made to validate the model's ability to accurate scouring analysis. Specific consideration has to be paid on the mesh resolution and turbulence model features that may affect the results.

5.2 Recommendation

In general, the scouring process at the end of SB is studied widely through field observing and by laboratory and CFD approaches. The effect of appurtenances on the minimizing of local scour could be studied in more detail. The design geometry of each appurtenance will be investigated to find the best type that reduces the scouring. The recommendation for the future researchers

1-Using $k{-}\varepsilon$ turbulent model instead of the RNG k-ε model in the Flow-3D software to simulate the scouring process in order to know which model has high accuracy in simulating scour process.

2-Instead of using Flow-3D for simulating the scouring process another CFD program will be used such as ANSYS and Fluent then results for both numerical and experimental will be compared.

3-In this study, only the sill geometry effect on the maximum scour depth was observed in the specified location, but in the future study, the location of the intermediate sill will be investigated to find the best location of the intermediate sill that reduces the scour to the minimum value for the same sill geometry.

4-The gap between impact wall and basin floor will be tested to find the best height of the gap that is minimizing the scour depth.

REFERENCES

Abdelhaleem, F. S. F. (2013). Effect of semi-circular baffle blocks on local scour downstream clear-overfall weirs. *Ain Shams Engineering Journal*, **4**(4), 675-684.

Acharya, A. (2011). Experimental study and numerical simulation of flow and sediment transport around a series of spur dikes. The University of Arizona.

Ali, A. M., & Mohamed, Y. A. (2010). Effect of stilling basin shape on the hydraulic characteristics of the flow downstream radial gates. *Alexandria Engineering Journal*, **49**(4), 393-400.

Annandale, G. W. (1995). Erodibility. *Journal of hydraulic research*, **33**(4), 471-494.

Bagnold, R. A. (1956). The flow of cohesion less grains in fluids. *Philosophical Transactions of the Royal Society of London A: Mathematical, Physical and Engineering Sciences,* **249**(964), 235-297.

Barlock, R. R. (2013). Stilling basin scour remediation using air injection and flat plate extension (Michigan Technological University).

Bradley, J. N., & Peterka, A. J. (1957). The hydraulic design of stilling basins: hydraulic jumps on a horizontal apron (basin i). *Journal of the Hydraulics Division,* **83**(5), 1-24.

Brethour, J. (2003). Modeling sediment scour. *Flow Science, Santa Fe, NM.*

Breusers, H. N. C. (1966). Conformity and time scale in two-dimensional local scour.

Breusers, H. N. C., & Raudkivi, A. J. (1991). Scouring, hydraulic structures design manual. *IAHR, AA Balkema, Rotterdam,* **143**.

Breusers, H. N. C., Nicollet, G., & Shen, H. W. (1977). Local scour around cylindrical piers. *Journal of Hydraulic Research*, **15**(3), 211-252.

Chabert, J., & Engeldinger, P. (1956). Etude des affouillements autor des piles depoints (Study of scour at bridge piers). *Bureau central d'Etudes les Equipment d'OutreMer, Laboratory National d'Hydraulique, France*.

Cheremisinoff, P.N., Cheremisinoff, N.P. and Cheng, S.L. 1987. Hydraulic mechanics 2. Civil Engineering Practice, *Technomic Publishing Company, Inc., Lancaster,Pennsylvania*, U.S.A. 780 p.

Chrisohoides, A., Sotiropoulos, F., & Sturm, T. W. (2003). Coherent structures in flat-bed abutment flow: Computational fluid dynamics simulations and experiments. *Journal of Hydraulic Engineering*, **129**(3), 177-186.

Ebrahim Nohani., Heydarnejad, M. 2014. Experimental Investigation of the Effect of Flow Angle of Attack on the Rate of Scour around the Slotted Bridge Pier at Different 55 Levels of River Bend. *IJRASET-International Journal for Research in Applied Science & Engineering Technology*, **2** (12):276-282.

Einstein, H. A. (1950). The bed-load function for sediment transportation in open channel flows (**Vol. 1026**). Washington DC: US Department of Agriculture.

Engelund, F., & Hansen, E. (1967). A monograph on sediment transport in alluvial streams. *Technical University of Denmark 0stervoldgade 10, Copenhagen K.*

Flow Science, Inc., (2012). FLOW-3Dv10-1-user-manual, *flow science, inc,santa Fe.*
USACE, U., (1992). Army Corps of Engineers. *CECW-ED-D Engineer Manual 11102-1603* .

Garde, R., Subramanya, K. S., & Nambudripad, K. D. (1961). Study of scour around spur-dikes. *Journal of the Hydraulics Division*, **87**(6), 23-37.

Gardes, R. A. (1986). *U.S. Patent No. 4,599,172. Washington, DC: U.S. Patent and Trademark Office.*

Gaudio, R., & Marion, A. (2003). Time evolution of scouring downstream of bed sills. *Journal of hydraulic research*, **41**(3), 271-284.

Gehlot, B. K., & Tiwari, H. L. (2014). Critical review of stilling basin models for pipe outlet works. *International Journal of Research in Engineering and Technology, eISSN*, 2319-1163.

Gilbert, G. K., & Murphy, E. C. (1914). The transportation of debris by running water (No. 86). *US Government Printing Office*.

Henderson, F. M. (1966). Open Channel Flow, **522**. *McMillan, New York*.

Hirt, C.W. and Nichols, B.D., (1981), Volume of Fluid (VOF) Method for the Dynamics of Free Boundaries, *Journal of Computational Physics* **39**, 201, 1981.

Hoffmans, G. J. C. M. (1990). Concentration and flow velocity measurements in a local scour hole. *Report no.* 4-90.

Hoffmans, G. J., & Pilarczyk, K. W. (1995). Local scour downstream of hydraulic structures. *Journal of Hydraulic Engineering*, **121**(4), 326-340.

Hopfinger, E. J., Kurniawan, A., Graf, W. H., & Lemmin, U. (2004). Sediment erosion by Görtler vortices: the scour-hole problem. *Journal of Fluid Mechanics*, **520**, 327-342.

Hydraulics Division, Proceedings of the American Society of Civil Engineers, **95**(6):1919-1941.

International Commission on Large Dams (ICOLD), *Spillways for Dams*, Bulletin 58, ICOLD,

Johnson, P. A. (2005). Preliminary assessment and rating of stream channel stability near bridges. *Journal of Hydraulic Engineering*, **131**(10), 845-852.

Kayaturk, S. Y. (2005). Scour and scour protection at bridge abutments (Doctoral dissertation, Ph. D. thesis, *Department of Civil Engineering, Middle East Technical University (METU), Ankara,Turkey*).

Khalifa, M. A., & Zahra, K. A. (2014). Collective Review in Particular Reference to Soil Erosion around Maritime Structures, Effects of the Angle of Wave: Attack on Coastal Areas Formation and Variation on Transport Rates. *American Journal of Marine Science*, **2**(1), 25-32.

Krishnappan, B. G., & Lau, Y. L. (1986). Turbulence modeling of flood plain flows. *Journal of hydraulic engineering*, **112**(4), 251-266.

Kuhnle, R. A., Jia, Y., & Alonso, C. V. (2008). Measured and simulated flow near a submerged spur dike. *Journal of Hydraulic Engineering*, **134**(7), 916-924.

Laursen E M 1952 Observations on the nature of scour. *Proc. 5th Hydraul. Conf.*: 179–197

Mastbergen, D. R., & Van Den Berg, J. H. (2003). Breaching in fine sands and the generation of sustained turbidity currents in submarine canyons. *Sedimentology*,**50**(4), 625-637.

Mays, L. W. (Ed.). (1999). Hydraulic design handbook. McGraw-Hill Professional Publishing.

Melville, B. W. (1984). Live-bed scour at bridge piers. *Journal of Hydraulic Engineering*, **110**(9), 1234-1247.

Melville, B. W., & Coleman, S. E. (2000). *Bridge scour*. Water Resources Publication.

Melville, B. W., & Raudkivi, A. J. (1977). Flow characteristics in local scour at bridge piers. *Journal of Hydraulic Research*, **15**(4), 373-380.

Mohammed, T. A., Noor, M. M. M., Huat, B. K., Ghazali, A. H., & Yunis, T. S. (2004). Effect of curvature and end sill angle on local scouring at downstream of a spillway. *International Journal of Engineering and Technology*, **1**(1), 96-101.

Morales, R., & Ettema, R. (2012). Insights from depth-averaged numerical simulation of flow at bridge abutments in compound channels. *Journal of Hydraulic Engineering*, **139**(5), 470-481.

Naot, D., Nezu, I., & Nakagawa, H. (1993). Calculation of compound-open-channel flow. *Journal of Hydraulic Engineering*, **119**(12), 1418-1426.

Negm, A. A. M. (2004, April). Effect of sill arrangement on maximum scour depth downstream of abruptly enlarged stilling basins. In *Hydraulics of Dams and River Structures: Proceedings of the International Conference, Tehran, Iran, 26-28 April 2004* (p. 181). CRC Press.

Nichols, B. D., & Hirt, C. W. (1975, October). Methods for calculating multi-dimensional, transient, free surface flows past bodies. In *Proc., 1st Int. Conf. Ship Hydrodynamics* (pp. 253-277). Naval Ship Research and Development Center, Bethesda, Md.

Novak, P., Moffat, A. I. B., Nalluri, C., & Narayanan, R. (2007). *Hydraulic structures*. CRC Press.

Olukanni, D. O., Adedeji, A. A., & Salami, A. W. (2017). Assessment of Selected Dams in Kwara State, Nigeria. *Journal of Research Information in Civil Engineering*, **14**(2), 1561-1573.

Özalp, M. C., & Bozkuş, Z. (2013). Experimental investigation of local scour around bridge pier groups (Doctoral dissertation, M. Sc. thesis, Department of Civil Engineering. The graduate School of Natural and Applied Sciences of Middle East Technical University.

Papanicolaou, A. T. N., Elhakeem, M., Krallis, G., Prakash, S., & Edinger, J. (2008). Sediment transport modeling review—current and future developments. *Journal of Hydraulic Engineering*, **134**(1), 1-14. Paris, 1987.

Peterka, A. J. (1958). Hydraulic design of stilling basins and energy dissipators.

Pezzinga, G. (1994). Velocity distribution in compound channel flows by numerical modeling. *Journal of Hydraulic Engineering*, **120**(10), 1176-1198.

Plaza, S., Potvin, A., & Sahab, A. Stilling Basins CIVE 401 Hydraulic Engineering Term Paper.

Prinos, P. (1990). Turbulence modeling of main channel-floodplain flows with an algebraic stress model. In *Proc. Conf. River Flood Hydraulics* (pp. 173-185).

Pritchard, R. W. (2013). 2011 to 2012 Queensland floods and cyclone events: Lessons learnt for bridge transport infrastructure. *Australian Journal of Structural Engineering*, **14**(2), 167-176.

Raudkivi, A. J. (1967). Analysis of resistance in fluvial channels. *Journal of the Hydraulics Division*.

Raudkivi, A. J. (1998). Loose boundary hydraulics. CRC Press.

Raudkivi, A.J. 1998. Loose boundary hydraulics. 4th Edition. Rotterdam ; Brookfield, VT : *Balkema*. 496 p.

Richardson, E. V., & Davies, S. R. (1995). Evaluating scour at bridges. Rep. *No. FHWA-IP-90-017 (HEC 18).*

Saleh, O. K., Negm, A. M., & Ahmad, N. G. (2003, April). Effect of asymmetric side sill on scour characteristics downstream of sudden expanding stilling basins. In *Al-Azahr Engineering 7th International Conference. Cairo Egypt*.

Saleh, O. K., Negm, A. M., Waheed-Eldin, O. S., & Ahmad, N. G. (2003, January). Effect of end sill on scour characteristics downstream of sudden expanding stilling basins. In *Proc. of 6th Int. Conf. On River Eng., Ahvaz, Iran* (pp. 28-30).

Publ. 12, p. 84-115. Shen, HW, VR Schneider, AND S. Karaki, 1969, Local scour around bridge piers: Am. Soc. Civil Engineers, *Jour. Hydraulics Div*., Vol. **95**, no. HY6, p. 1919-1940.

Shields, A. (1936). Application of similarity principles and turbulence research to bed-load movement. *CalTech library*.

Staplin, L., Lococo, K., Byington, S., & Harkey, D. (2001). Highway design handbook for older drivers and pedestrians (No. FHWA-RD-01-103,).

TAREQ, M. Experimental Study of Local Scour Downstream of Cylindrical Bridge Piers.

Tiwari, H. L., & Goel, A. (2014). Effect of end sill in the performance of stilling basin models. *American Journal of Civil Engineering and Architecture*, **2**(2), 60-63.

Tiwari, H. L., & Goel, A. (2016). Effect of impact wall on energy dissipation in stilling basin. *KSCE Journal of Civil Engineering*, **20**(1), 463-467.

Tiwari, H. L., Gahlot, V. K., & Sharma, A. (2014). Effect of Intermediate Sill on the Performance of Stilling Basin Model. *International Journal of Scientific Engineering and Technology*, **3**(4), 414-417.

Tiwari, H. L., Gahlot, V. K., & Tiwari, S. (2013). Reduction of scour depth downstream of pipe outlet stilling basin using end sill. *International Journal of Engineering Sciences*, **2**(7), 20-25.

Tiwari, H. L., Gehlot, V. K., & Tiwari, S. Effect of height of triangular siil on the performance of stilling basin model.

U.S. Bureau of Reclamation (USBR), *Design of Small Dams*, U.S. Bureau of Reclamation, Denver,CO, 1987.

USACE, U., (1992). Army Corps of Engineers. *CECW-ED-D Engineer Manual 1110-2-1603* .

Van Rijn, L. C. (1993). Principles of sediment transport in rivers, estuaries and coastal seas (Vol. **1006**). Amsterdam: Aqua publications.

Van Rijn, L. C. (2013). Local scour near structures. *Taken from: www. leovanrijnsediment. com*.

VRIES, D. (1973). Application of physical and mathematical models for river problems. in: general reports, discussions, lectures, VOL. **IV**.

Wei, C. Y., & Lindell, J. E. (1999). Hydraulic design of stilling basin and energy dissipators. *Hydraulic Design Handbook. Chicago, IL, USA: McGraw-Hill*, 18-1.

Xie, Z. (2011). Theoretical and numerical research on sediment transport in pressurized flow conditions. The University of Nebraska-Lincoln.

Yakhot, V., & Orszag, S. A. (1986). Renormalization group analysis of turbulence. I. Basic theory. *Journal of scientific computing*, **1**(1), 3-51.

Yildiz, B. (2014). Time evolution of the flow characteristics around bridge abutments during scouring process (doctoral dissertation, middle east technical university).

Zaghloul, N. A. (1983). Local scour around spur-dikes. *Journal of Hydrology*, **60**(1-4), 123-140.

Zhang, Z., Ersoz, E., Lai, C. Q., Todhunter, R. J., Tiwari, H. K., Gore, M. A., & Buckler, E. S. (2010). Mixed linear model approach adapted for genome-wide association studies. *Nature genetics*, **42**(4), 355-360.